



NTNU – Trondheim
Norwegian University of
Science and Technology

Structural Interpretation and Investigation of the Displacement Gradients of the Normal Fault System beneath the Horda Platform, the northern North Sea

Kwanjai Kaenmee

Petroleum Geosciences

Submission date: July 2012

Supervisor: Egil Tjøland, IPT

Co-supervisor: Giulio Viola, IGB
Per Terje Osmundsen, NGU

Norwegian University of Science and Technology
Department of Petroleum Engineering and Applied Geophysics



NTNU

Norwegian University of
Science and Technology

Structural Interpretation and Investigation of the Displacement Gradients of the Normal Fault System beneath the Horda Platform, the northern North Sea

Submitted by

Kwanjai Kaenmee

Supervised by

Egil Tjøland

Per Terje Osmundsen

Giulio Viola

TPG4925 Petroleum Geosciences, Master Thesis (Spring 2012)

Department of Petroleum Engineering and Applied Geophysics,

Faculty of Engineering Science and Technology

Acknowledgements

First of all, I would like to offer my gratitude to my supervisor, Associate Professor Egil Tjøland (IPT), for his advice and support throughout the work and help in the data preparation. My sincere appreciation goes to Per Terje Osmundsen (NGU) for his great technical knowledge, guidance, suggestions and idea to complete my thesis. My thanks also go to Professor Giulio Viola (IGB) for the valuable assistance and help in the preparation of the report, and Knut Backe for the help to download the data from PetroBank into the system.

I would also like to acknowledge the financial support of the PTTEP, my company in Thailand, and the Geology Management Team of the PTTEP for giving me the opportunity to continue my study in the master degree in NTNU.

The Department of Petroleum Engineering and Applied Geophysics has provided the support and equipment I have needed to produce and complete my thesis.

Last but not least, I am thankful to my parents and other members of my family for the inspirations to study abroad and to continue acquiring knowledge. I am grateful to friends in Thailand, Trondheim and elsewhere and Bangkok Cafe for making my life happy and joyful in Trondheim, and my last appreciation goes to Fermín for his support and being by my side.

Abstract

The North Sea basin is one of the best-studied areas in the world with respect to the structural and sedimentary architecture of rift zones. The Base Cretaceous Unconformity, which defines a mappable horizon at the transition from synrift to postrift sequences associated with the Jurassic–Cretaceous rift, is well known as a reference marker for both seismic and well log interpretations and covers most of the basin. This unconformity is interpreted at the locations of the Øygarden Fault Zone, the Troll Fault Block, the North Viking Graben, the Tampen Spur, the Snorre Fault Block, the Sogn Graben and the Horda Platform. The complexities of the unconformity have been established and vary with the structural and geographical position within the basin. However, as the Base Cretaceous Unconformity covers most of the northern North Sea, its structural time map, is used to derive the picture of post-structural framework of a rift basin and to locate essential structures in the deeper sections.

Three main reflectors (Pre-Jurassic 1, Pre-Jurassic 2 and Top seismic basement) located beneath the Base Cretaceous Unconformity on the Horda Platform, and have been interpreted using 2D seismic reflection data. These three reflectors have been studied in order to investigate in detail the displacement gradients and possible linkage of the early fault system under the Horda Platform, and to evaluate their effect on the large-scale sediment architecture. A main reason to work on the structures under the Horda Platform is due to the fact that these structures are believed to have existed already in the early stages of the northern North Sea basin development.

The extensional normal fault systems of both the Permo-Triassic and the Late Jurassic rifts are considered a key control on the geological structures and sedimentary architecture of the region as presently seen. The basin evolution related Permo-Triassic rifting is most pronounced on the eastern part of the Horda platform where its synrift geometry is obviously seen with the huge segment length and largest uplift explainable by a flexural stretching model. The rift axis is transferred to position at base of the Viking graben during the Late-Jurassic rifting with the smaller magnitude of extension than the Permo-Triassic as clearly seen by the less thickness of the synrift geometry. However, the structural evolution of normal faults and the basin architecture under the Horda Platform is particularly affected by the complex interaction of fault linkage, fault propagation, fault growth, and death of fault through times from the early stage to the final stage of the basin development. Apart from the effects of major tectonic controls, additionally, non-tectonic parameters, such as climate, sea or lake level changes, and differences in amount and type of sediment supply, should be taken into account to influence the stratigraphic and sedimentation patterns in the basin.

Contents

Acknowledgements.....	i
Abstract.....	ii
Contents.....	iii
List of Table and Figures.....	v
1. Introduction.....	1
1.1 Objectives of the study.....	1
1.2 Location of the study area.....	1
1.3 Structural framework of the northern North Sea.....	3
1.4 Relations between normal faulting and basin sedimentation in rift.....	8
2. Two-dimensional (2D) seismic data and study methodology.....	13
2.1 Seismic reflection data	13
2.2 Study methodology.....	13
3. Base Cretaceous Unconformity interpretation	19
3.1 Seismic interpretation.....	20
3.2 Complexity of the Base Cretaceous Unconformity.....	27
3.3 Mapping.....	28
4. Deep reflector interpretation.....	31
4.1 Pre-Jurassic 1.....	31
4.1.1 Seismic interpretation.....	31
4.1.2 Mapping.....	32
4.2 Pre-Jurassic 2.....	33
4.2.1 Seismic interpretation.....	33
4.2.2 Mapping.....	33
4.3 Top seismic basement.....	33
4.3.1 Seismic interpretation.....	33

4.3.2 Mapping.....	34
5. Discussion.....	36
5.1 Normal faulting and basin evolution.....	36
5.2 Stratigraphy and sedimentary architectures related to basin development.....	42
5.3 Deep structure.....	46
6. Conclusions.....	49
7. References.....	50

List of Table and Figures

Table 2.1 List of all selected lines for each interpreted reflector separately.....	15
Figure 1.1 Location of study area. Key structural elements are the Øygarden-Fault Zone, the North Viking Graben, the Tampen Spur, the Sogn Graben and the Horda Platform.....	2
Figure 1.2 Basin stratigraphy of the North Viking Graben and adjacent areas.....	3
Figure 1.3 Triassic rifting patterns.....	4
Figure 1.4 Jurassic rifting patterns.....	6
Figure 1.5 Map illustrating the evolution of the structural framework of the northern North Sea from the Triassic to the Cretaceous.....	7
Figure 1.6 Fault-displacement gradient controls the first-order geometry of a half-graben (rift basin).....	8
Figure 1.7 Schematic evolution of three fault segments to produce a major border – fault zone.....	9
Figure 1.8 An example of significant lateral variation of localised uplift and – subsidence around a schematic segmented normal fault zone.....	10
Figure 1.9 Mode of rotation in (a) synrift and (b) post-rift stages. (c) rift-basin – configuration.	11
Figure 1.10 Sketch showing different configurations of BCU in the central basin and – in the sub-platform and platforms.....	12
Figure 2.1 Selected 2D seismic lines for the interpretation of the BCU.....	16
Figure 2.2 Selected 2D seismic lines for interpreting Pre-Jurassic 1, Pre-Jurassic 2 and- Top seismic basement and location of well 31/6-1.....	17
Figure 2.3 Example of the framework used for horizon interpretation.....	17
Figure 2.4 Example of fault polygon generation.....	18

Figure 3.1 Simple sketches of unconformity. A.) Disconformity, B.) Nonconformity – and C.) Angular unconformity.....	19
Figure 3.2 Illustration of the concept built in the “Flatten horizon” tool to locate the- BCU across rotated fault blocks along the 2D seismic line NVGTI92-106.....	21
Figure 3.3 NVGT88-06 reference seismic section for Base Cretaceous Unconformity.....	22
Figure 3.4 Illustration of the flat angular unconformity from 2D seismic line NVGT88-06..	23
Figure 3.5 Illustration of the faulted unconformity from 2D seismic line NVGT88-06.....	23
Figure 3.6 Illustration of the merging unconformity from 2D seismic line NVGT88-06.....	24
Figure 3.7 Illustration of the eroded fault block sequence from the 2D seismic line – NVGT88-06.....	24
Figure 3.8 Illustrations of the disconformity.....	25
Figure 3.9 Illustration of the disconformity, faulted unconformity and onlap features – from a graben area as seen in the 2D seismic line NVGT88-07.....	26
Figure 3.10 Illustration of the flat angular unconformity from the 2D seismic line- NVGT88-08.....	27
Figure 3.11 Illustrations of the faulted BCU and the eroded fault block crests from – the 2D seismic line NVGTI92-106.....	28
Figure 3.12 Examples of the complexity of the BCU.....	29
Figure 3.13 Structural time map of Base Cretaceous Unconformity.....	30
Figure 4.1 Illustration of interpretation of faults and seismic horizons in the Horda – Platform area from the reference 2D seismic line NVGT88-05.....	31
Figure 4.2 Structural time map of the Pre-Jurassic 1.....	32
Figure 4.3 Structural time map of the Pre-Jurassic 2.....	34
Figure 4.4 Structural time map of the top seismic basement with well 31/6-1.....	35
Figure 5.1 Structural time map of Top seismic basement and schematic cross-sections.....	37
Figure 5.2 Schematic 3D evolution of a normal fault array.....	38

Figure 5.3 Illustration of fault linkages.....	39
Figure 5.4 Structural framework in the northern North Sea.....	41
Figure 5.5 Simple illustration of sedimentary architectures in a rift basin from 2D – seismic line NVGT88-08.....	42
Figure 5.6 Triangular wedge geometry of synrift succession of the Permo-Triassic- rift from 2D seismic line NVGT88-05.....	43
Figure 5.7 An isochore map of succession from Top seismic basement to Pre- Jurassic 2.....	44
Figure 5.8 An isochore map of succession from Pre-Jurassic 2 to Pre-Jurassic 1.....	45
Figure 5.9 Simple illustration of detachment fault across the Central Graben, - southern North Sea based on regional seismic survey.....	46
Figure 5.10 Examples of the subsurface structures under the Horda Platform in the – northern North Sea from 2D seismic line NNST84-05.....	47
Figure 5.11 An example of the possible first rifting normal fault in the northern- North Sea from 2D seismic line NVGTI92-106.....	47
Figure 5.12 Simple illustration of fault development in rift basin.....	48

1. Introduction

This thesis work is submitted to the Norwegian University of Science and Technology (NTNU) for partial fulfillment of the requirements for the degree of Master of Sciences in Petroleum Geosciences.

The project has been carried out at the Department of Petroleum Engineering and Applied Geophysics, Faculty of Engineering Science and Technology, NTNU.

1.1 Objectives of the study

The goals of this thesis are listed below:

- To use seismic data of good quality to map the three-dimensional architecture of an extensional fault system and how this affected the large-scale basin architecture.
- To investigate the results of the interaction between the Permo-Triassic versus Jurassic rift phases in the Horda Platform area.
- To investigate in detail the displacement gradients and linkage of the fault system under the Horda Platform.

1.2 Location of the study area

The study area is located in the northern North Sea sedimentary basin (Figure 1.1). It is situated approximately at latitude 59°- 62°N and longitude 2°-4°30'E, which is to the west of Bergen along the Norwegian coast. The study area covers more than 30,000 km². Major gas and oil fields in the study area are the Troll field, one of the biggest gas field in the North Sea, the Snorre field and the Gullfalks field. The area includes several distinct structural elements within the greater Viking Graben, that is, the Øygarden Fault Zone, the Troll Fault Block (in the thesis often referred to as the northern part of the Horda Platform), the North Viking Graben, the Tampen Spur (sometimes specifically mentioned as the Snorre Fault Block of the Snorre oil field), the Sogn Graben and the Horda Platform.

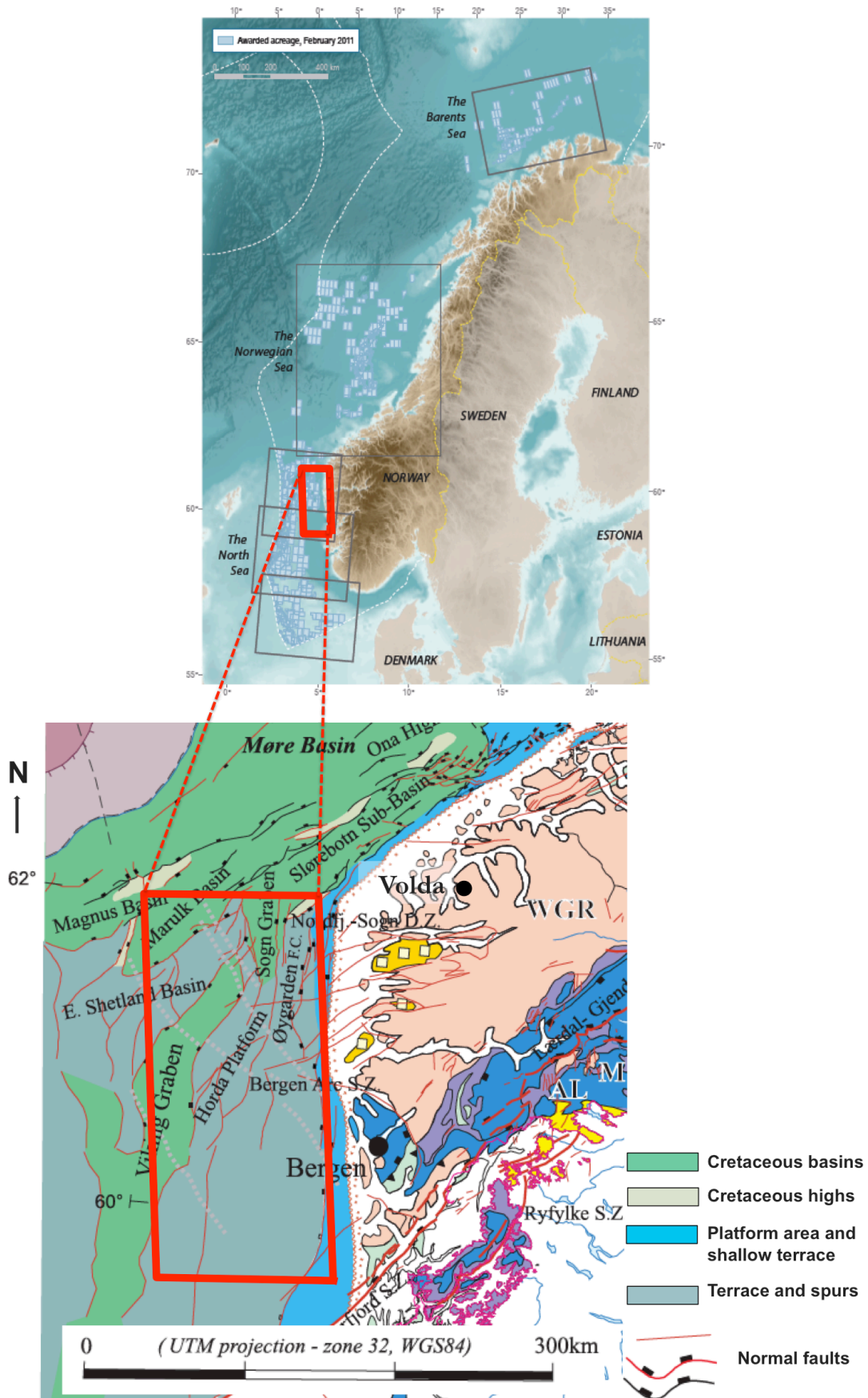


Figure 1.1 Location of study area. Key structural elements are the Øygarden Fault Zone, the North Viking Graben, the Tampen Spur, the Sogn Graben and the Horda Platform (modified from the Norwegian Petroleum Directorate and Mosar et al., 2002)

1.3 Structural framework of the northern North Sea

The northern North Sea rift basin is a failed rift system, which underwent two important episodes of lithospheric extension during the late Permian-earliest Triassic (?) (in this thesis referred to as the Permo-Triassic event) and the Mid-Jurassic to earliest Cretaceous (here referred to as the Late Jurassic event), respectively (Figure 1.2; Christiansson et al., 2000). The details of each rift and the postrift successions are discussed separately in the following sections.

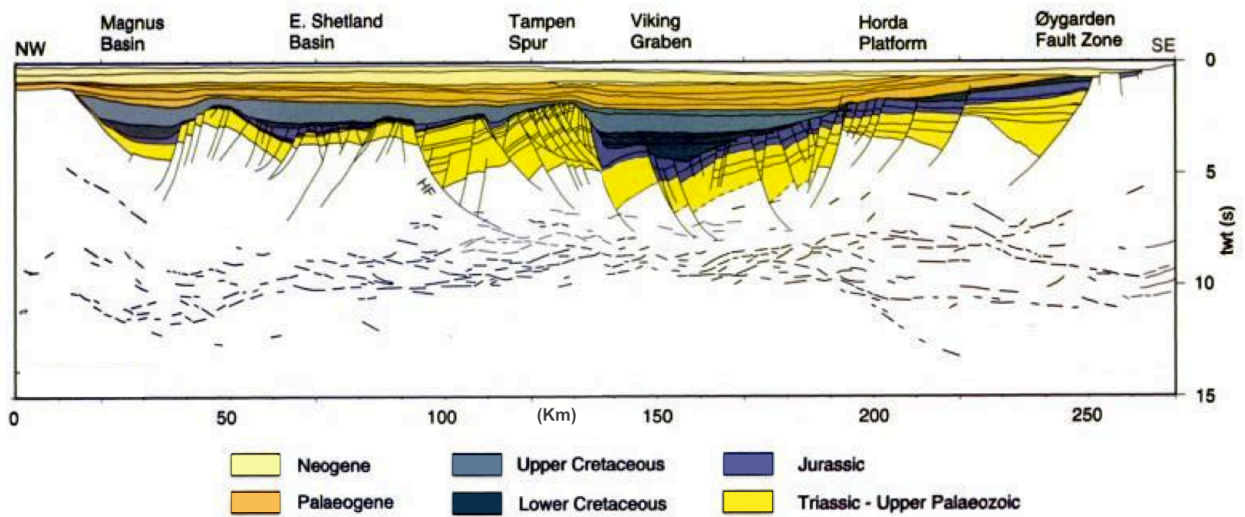


Figure 1.2 Basin stratigraphy of the North Viking Graben and adjacent areas. The Permo-Triassic rift is displayed by yellow fault blocks whereas the Late Jurassic rift is displayed by violet and dark green fault blocks (modified from Christiansson et al., 2000)

I) Permo-Triassic rift event:

The axis of the Permo-Triassic rift is believed to be centered beneath the present Horda Platform (Figure 1.3), coincident with a pre-Triassic half-graben on top of the crystalline basement (Christiansson et al., 2000). The effects of the Permo-Triassic rifting are preserved within the marginal areas of the Viking Graben, where the overprinting effects of the later Jurassic-Cretaceous rifting were recorded the least. Predominantly north-south structures, e.g. north-south striking rotated fault blocks and asymmetric half-grabens, characterize the Permo-Triassic rift (Coward et al., 2003). The structures within the northern North Sea rift basin are bounded by the Øygarden Fault Zone in the east and the East Shetland Platform in the west. Christiansson et al. (2000) presented evidence in favour of these areas being tectonically active during the early Permo-Triassic rifting stage. This is based on Devonian and older sediments from a few wells in East Shetland. Although no wells reached the sediments in pre-Triassic half-grabens beneath the Horda Platform, there are reasons to believe that Devonian sediments are present there as well (Christiansson et al., 2000).

II) Late Jurassic rift:

Jurassic rifting began in late Mid-Jurassic times and peaked in Late-Jurassic time (Christiansson et al., 2000). The rift axis for the Late Jurassic rift is believed to lie beneath the present Viking Graben (Figure 1.4). The extension direction in the northern North Sea was

initially east-west and mimicked the direction of the Permo-Triassic extensional regime, resulting in north-south elongated grabens. Later, the greatest extension direction rotated into a northwest-southeast direction, resulting in the prominent northeast-southwest trending North Viking Graben. It is not yet clear when the shift occurred, but it is possibly of mid-late Jurassic or early Cretaceous age (Christiansson et al., 2000).

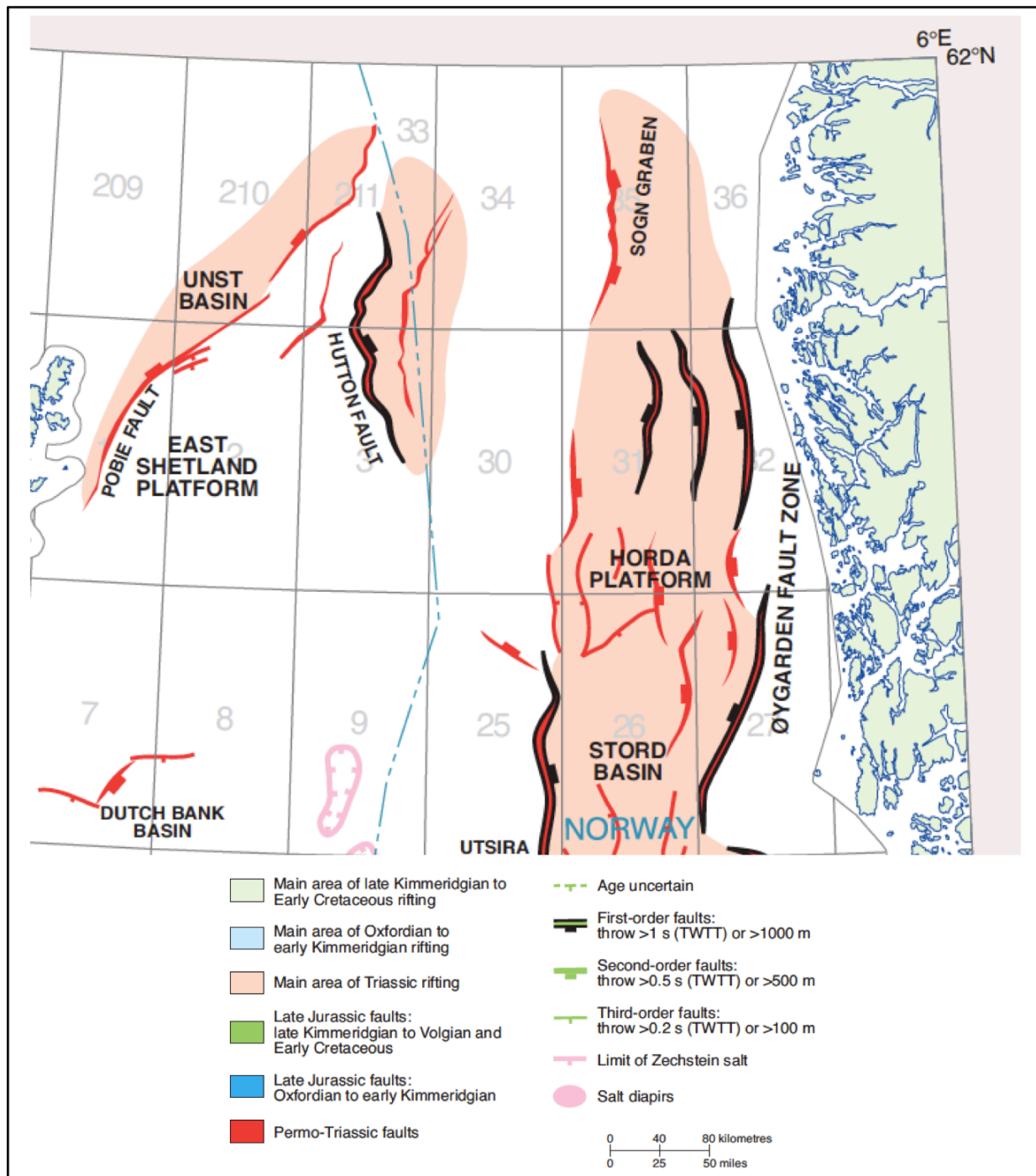


Figure 1.3 Triassic rifting patterns (from Zanella and Coward (2003))

The initial stages of the Jurassic rifting phase are thought to have impacted on the architecture of the graben more significantly than the final stages did due to the thermal cooling period of the Permo-Triassic episode and fault reactivations along the marginal basin. As a

consequence, the Viking Graben became broader, more pronounced and eventually developed a mature topography with platforms, sub-platforms, interior grabens, and graben feature along its axis (Christiansson et al., 2000). However, locally it is clearly seen that faulting continued well into the Cretaceous. This later activity is believed to have been mainly gravity-driven (Christiansson et al., 2000), wherein faulting was most commonly associated with the escarpments of the master faults along the basin margins. The northernmost Viking Graben and the Sogn Graben accommodated more extensive fault activity because of the influences from extensional faulting in the Møre Basin (Figure 2.14 in the Millennium Atlas (Coward et al., 2003)). In addition, localized structural inversion and uplift took place in the Viking Graben resulting in local thrust faults, which can be seen in seismic reflection data (Coward et al., 2003).

III) Cretaceous postrift

A phase of regional cooling following the Late Jurassic rift phase caused regional subsidence in the basins, resulting in deep-water conditions at the basin center. In the northern North Sea, normal faults were still active during the earliest Cretaceous with deposition of clastic sediments along the fault scarps, with onlap features terminated at erosional surfaces, particularly the Base Cretaceous Unconformity (Coward et al., 2003). The gradual infilling of the graben depression with deep-water sediments was accompanied by a rise in eustatic sea level. Hence, while the thick Upper Cretaceous chalk formed all over the southern and central North Sea, terrigenous mudstones governed the northern North Sea (Christiansson et al., 2000). The postrift sequences continued to accumulate in the basin areas, with the clastic component derived from uplifted areas in the north and west of the northern North Sea. The postrift succession can presently be observed as a relatively flat-lying sequence overlying the faulted synrift strata.

In a nutshell, the extensional normal faulting systems were repeatedly reactivated from the late Paleozoic to the late Mesozoic as summarized in Figure 1.5.

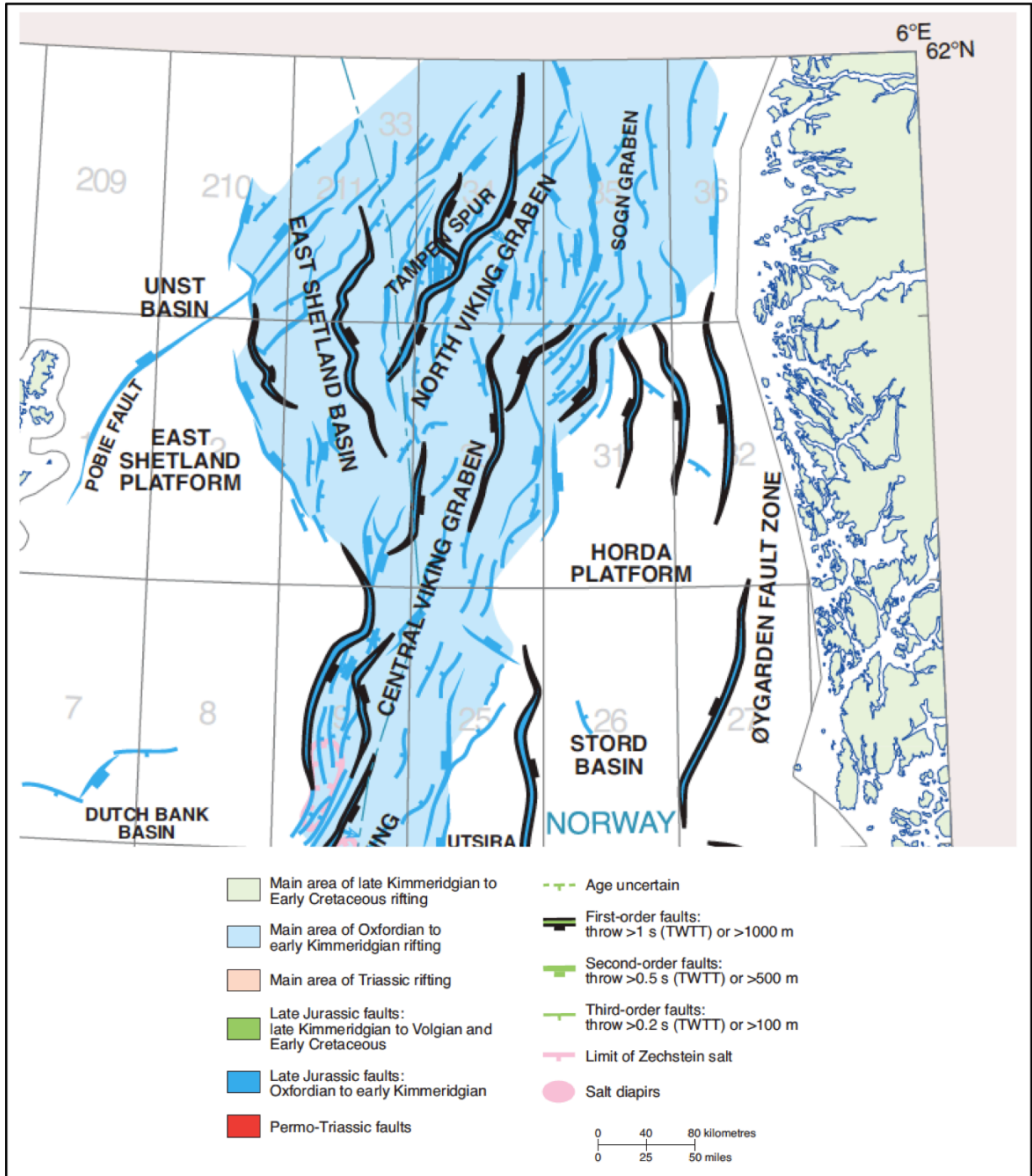


Figure 1.4 Jurassic rifting patterns (from Zanella and Coward, 2003)

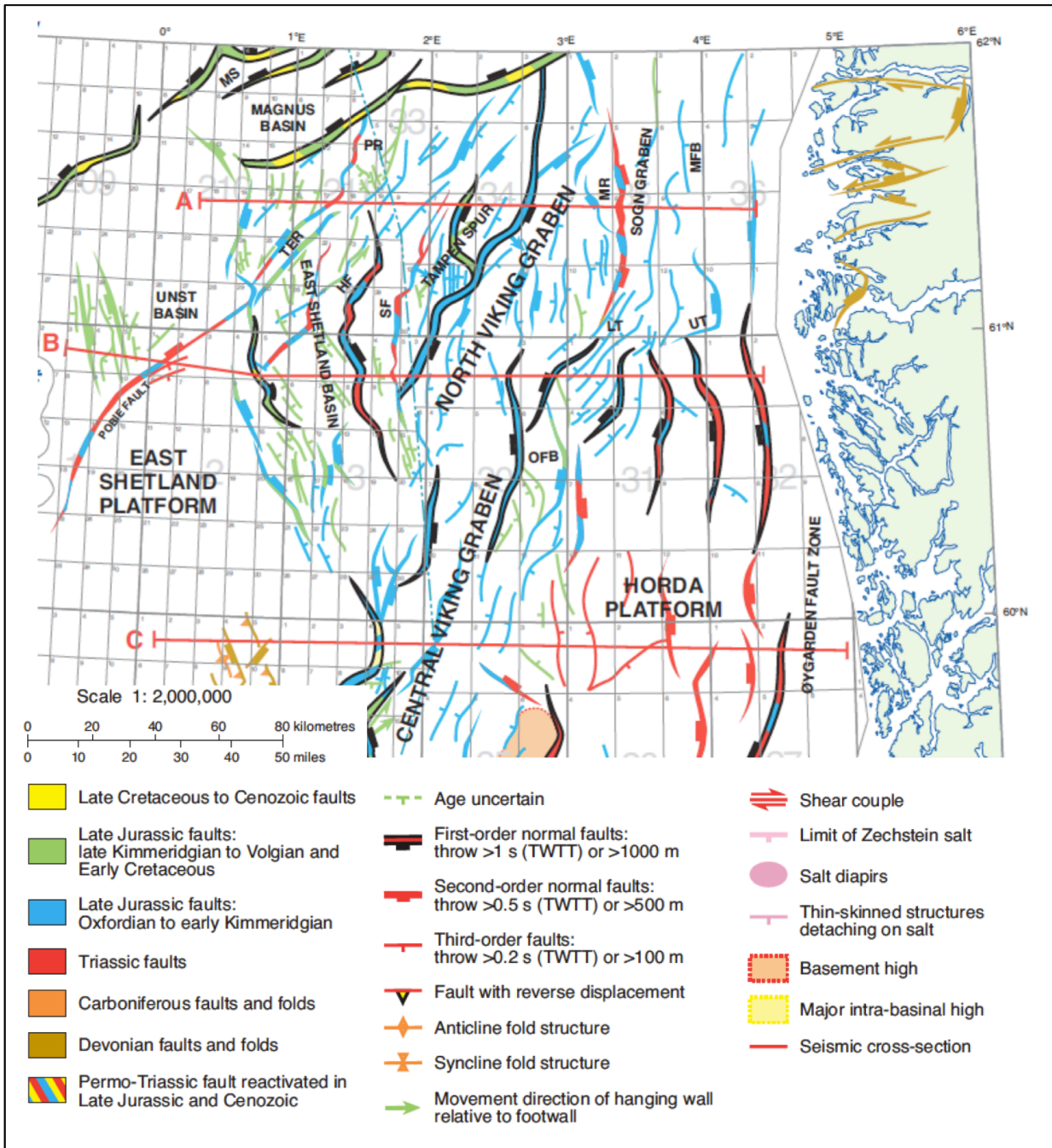


Figure 1.5 Map illustrating the evolution of the structural framework of the northern North Sea from the Triassic to the Cretaceous (from Zanella and Coward, 2003).

1.4. Relations between normal faulting and basin sedimentation in rifts

The classic architecture of a rift basin includes half-grabens bounded by normal faults. The half-graben geometry is controlled by the activity of extensional normal fault systems (Figure 1.6a below), wherein the greatest fault displacement ideally occurs along the central part of the fault and decreases progressively away from it (e.g. Gawthorpe et al., 1997). As a consequence, differential uplift of the footwall and subsidence of the hanging wall take place along the fault plane and synrift sediments are deposited overlying prerift sediments as illustrated in Figure 1.6b.

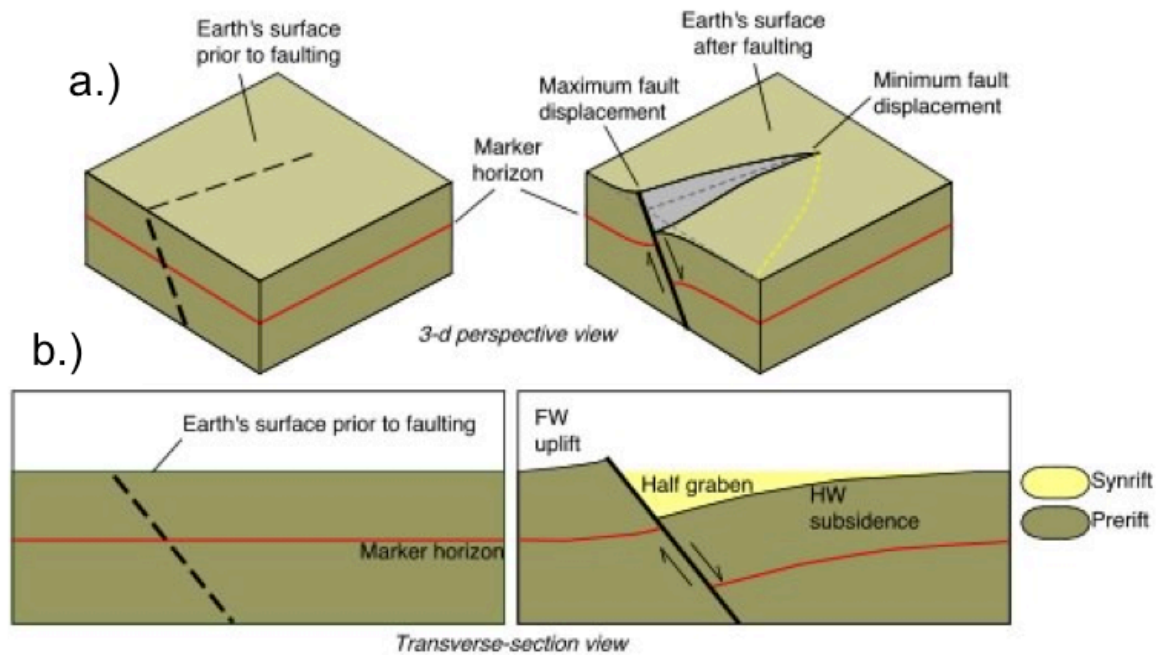


Figure 1.6 Fault-displacement gradient controls the first-order geometry of a half graben (rift basin). a.) Top view representing the situation before (left) and after (right) faulting along the half-graben bounding normal fault. b.) Cross section before (left) and after (right) faulting and sedimentation showing footwall uplift and hanging wall subsidence. The latter produces a wedge-shaped basin (half graben). Figure taken from Lamont -Doherty Earth Observatory, Columbia University webpage.

Gawthorpe and Leeder (2000) discussed a simple relationship between fault length and displacement in order to describe fault evolution, growth through time and interaction between different fault segments. Namely, the proposed scaling relationship between displacement and length is $D=cL^n$ where D is the maximum displacement along the fault scarp, L is the maximum trace length, c is a constant related to the rock properties of the rock system being faulted and n varies from 1 to 2. The possible evolution of three initially isolated fault segments to create one major fault is shown in Figure 1.7. Isolated and small faults are present in the initial stage (Figure 1.7A). In Figure 1.7B, two faults start to join resulting in a larger bulk fault displacement (D) of fault B, and three segments eventually link. The final linkage has also severed consequences on the development of the local topography and in detail it creates depressed zones, indicated by red arrows, at the former relay zones. Moreover, the scatter in the $D-L$ relationship as seen in all three stages of Figure 1.7 reflects fault growth by segment linkage (Gawthorpe and Leeder, 2000).

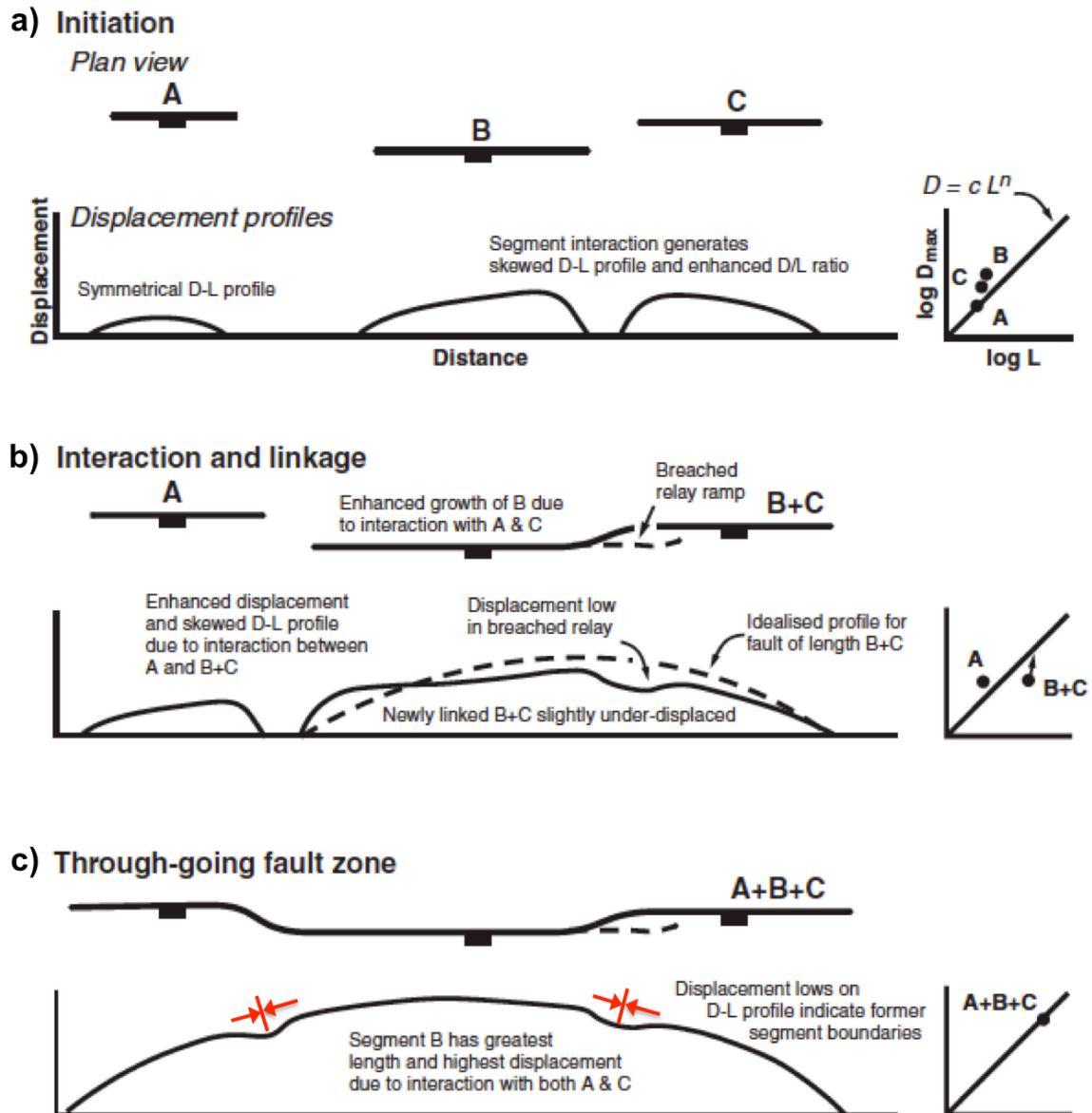


Figure 1.7 Schematic evolution of three fault segments to produce a major border fault zone, (a) Fault initiation stage, (b) interaction and linkage stage, (c) through-going fault zone stage (modified from Gawthorpe and Leeder, 2000).

Gawthorpe et al. (1994) suggested that five key parameters control stratigraphy and sedimentation patterns: (i) eustatic sea level; (ii) tectonic subsidence/uplift; (iii) sediment supply; (iv) climate; and (v) basin physiography. In particular, the tectonic component is mainly associated with fault displacement, that is, footwall uplift and hanging wall subsidence are greatest at the centre of a fault segment and decrease towards the fault tips (Gawthorpe et al., 1994). This results in high footwall elevation and low hanging wall elevation in the centre of fault segments (Figure 1.8). According to Figure 1.8, location 1, situated in the centre of a fault, shows the greatest subsidence. In contrast, location 5, situated on the hanging wall dip slope, and location 3, situated at the tip of the fault segment, present lower subsidence. Location 2 shows the largest uplift at the center of the fault segment and location 4 has zero uplift or subsidence rates.

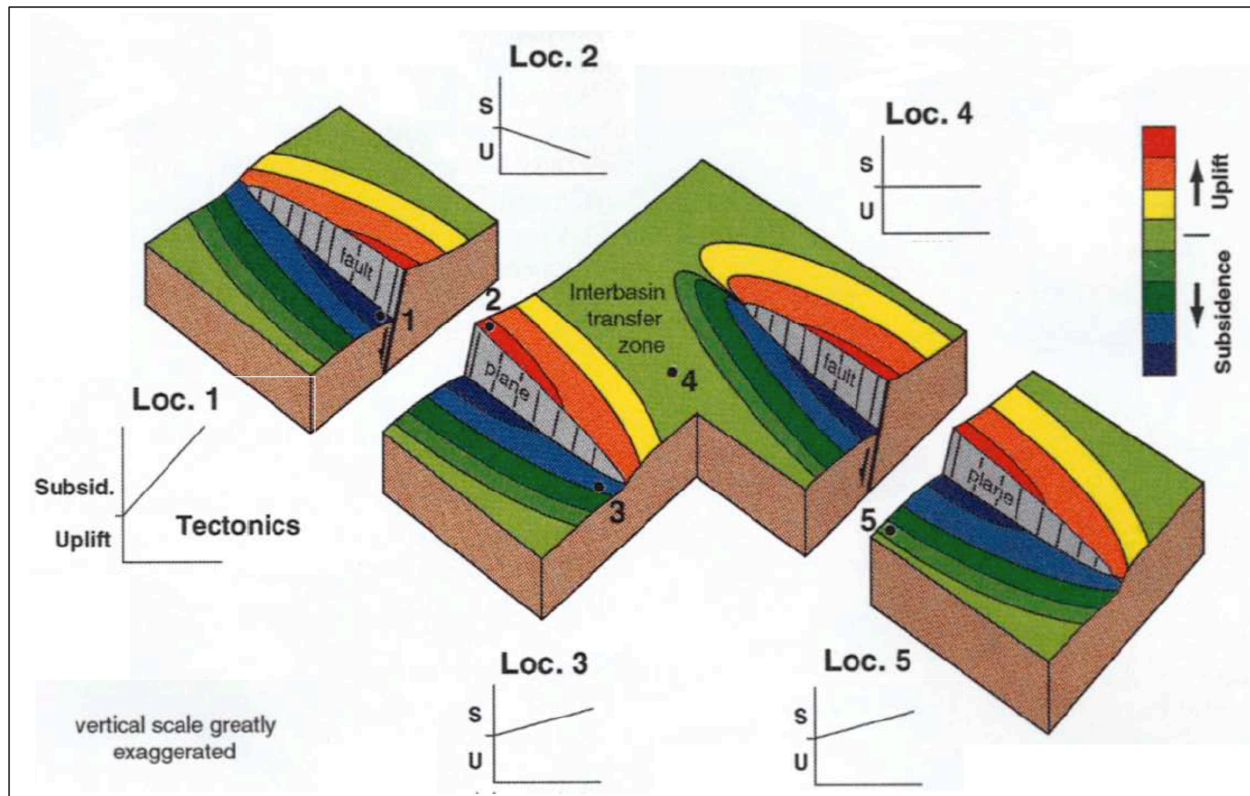


Figure 1.8 An example of significant lateral variation of localised uplift and subsidence around a schematic segmented normal fault zone. The amount of fault displacement and deformation decays away from the centre of the fault zone to the segment boundaries (transfer zone) and away from the fault zone. The variations in uplift or subsidence are shown in graphs for locations 1 to 5 in different structural locations.

The half-graben geometry described above is directly controlled by the deformation (displacement) field surrounding the boundary fault systems and is affected by fault propagation and forced folding (Gawthorpe et al., 1997). As displacement accumulates on the boundary fault, the basin deepens through time. Moreover, the basin widens through time because the width of the hanging-wall increases with increasing fault displacement, and the basin lengthens through time because the length of the fault increases with increasing displacement (Cowie, 1998).

The northern North Sea basin has a special horizon marker, which is an unconformity known as the Base Cretaceous Unconformity (BCU). The BCU covers most of the basin. Kyrkjebø et al. (2004) discussed the relation between different structural locations within the basin and across the sub-basins, for example, platform, sub-platform and rotated fault block, and internal graben, (Figure 1.9), and the different local character of the BCU (Figure 1.10). The definitions of each term are described below by text and are illustrated in Figure 1.10.

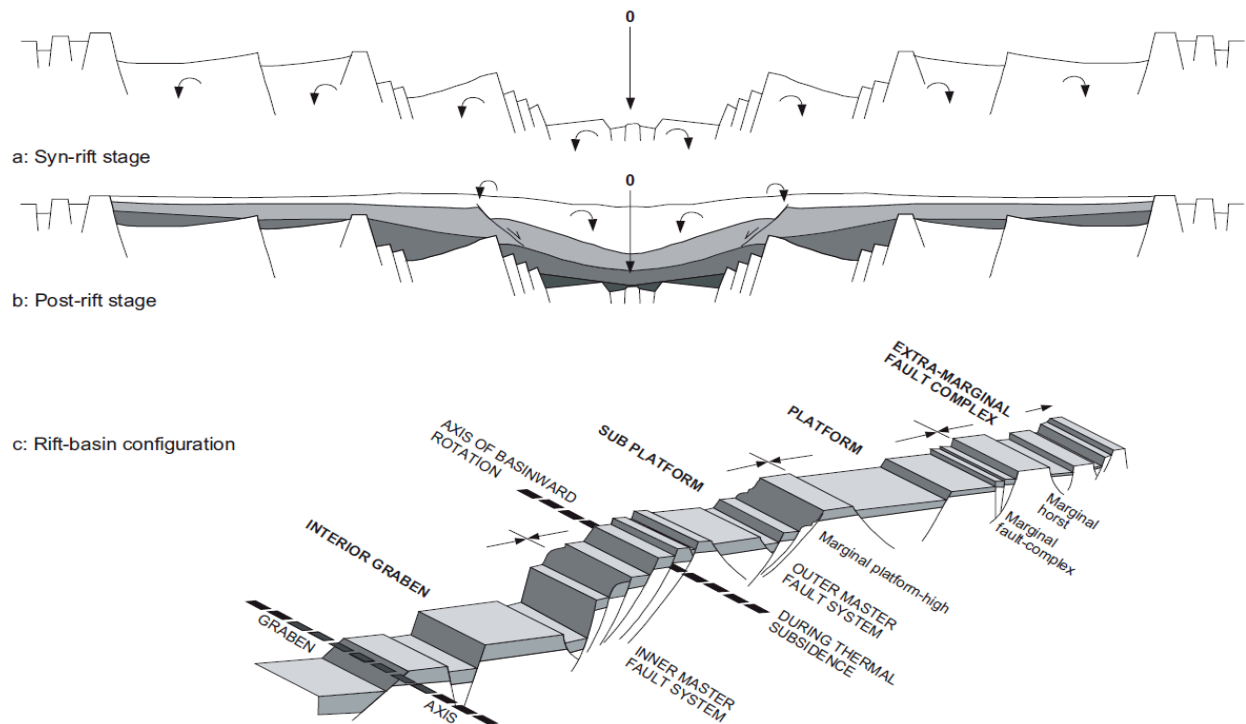


Figure 1.9 Mode of rotation in (a) synrift and (b) post-rift stages. (c) rift-basin configuration. From Kyrkjebø et al. (2004).

- A platform is generally the ancient and relatively stable segment of a continental craton composed of igneous or metamorphic rocks, and located where sediments and sedimentary rocks overlie the basement.

- A sub-platform is the term for the tectonic units that are situated structurally between the relatively stable platforms and the basin interiors. It is a relatively flat, horizontal or gently inclined surface of marine origin, mostly an old abrasion surface. Sub-platforms principally are bounded from the platform areas by the outer (synthetic) master fault system of the graben.

- Rotated fault blocks are located at the fronts of the sub-platforms and represent the morphologically most unstable and the tectonically most active setting in the basin. Rocks of these blocks are influenced by uplift as a result of fault-block rotation, elastic response of faulting, and isostatic adjustments (Kyrkjebø et al. 2004).

- An interior graben is fundamentally located between the sub-platforms and the axis of the master grabens. However, there are several grabens present also under the platform. It is normally a depressed segment and elongated block bounded by parallel faults along its two longest sides. An interior graben is fundamentally separated from the sub-platforms by a (synthetic) master fault system (Kyrkjebø et al. 2004).

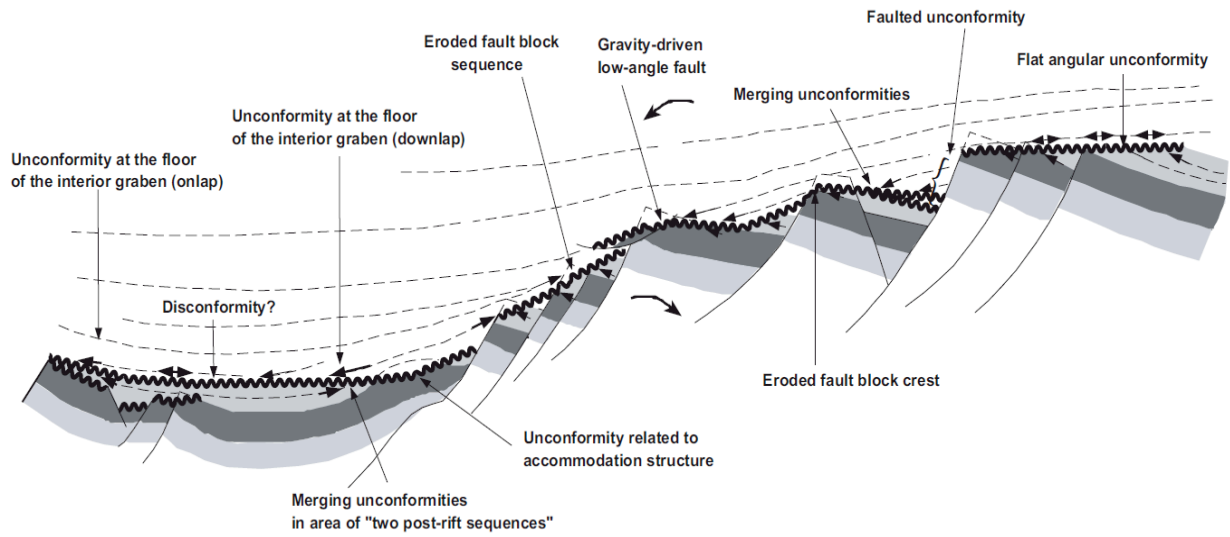


Figure 1.10 Sketch showing different configurations of BCU in the central basin and in the sub-platform and platforms. From Kyrkjebø et al. (2004).

2. Two-dimensional (2D) seismic data and study methodology

2.1 Seismic reflection data

Most of the 2D seismic reflection data used in this thesis work are data of public domain from PetroBank and part of the seismic data are from the Department of Petroleum Engineering and Applied Geophysics, Faculty of Engineering Science and Technology, NTNU. Each seismic dataset, for example, SH8001, NVGT88 and ST8201, has a different year of acquisition and processing. For instance, SH8001 was shot as a 2D seismic survey in 1980 (first two numbers after SH) and was processed twice, one in 1980 and another in 1992. The latest seismic processing year for each seismic dataset used was chosen in this thesis. A list of all selected lines is shown in Table 2.1.

2.2 Study methodology

Software/Application:

This work was carried out by using the software "Petrel" by Schlumberger, a commercial software package used worldwide by the oil and gas industry. The main applications used were the "seismic interpretation" and "make/edit surface", used to pick seismic reflectors. Unfortunately, the seismic well-tie tool was not available for correlating and calibrating interpreted horizons/faults to well logs. Therefore, this work has been done by using only 2D seismic data.

Horizon interpretation

Most of the selected horizons were interpreted manually because of difference in seismic resolutions for each seismic line. Four main reflectors and two additional reflectors were interpreted as listed below.

Main reflectors (Figure 1.2):

I) Base Cretaceous Unconformity (BCU): A major erosional surface, formed at the base of the Cretaceous succession, covers most of the northern North Sea, and shows a strong reflection on seismic section.

II) Pre-Jurassic 1: A horizon located at the top of the Permo-Triassic succession (i.e. the base of the Jurassic) on the Horda Platform, and shows a gently declined reflection beneath subparallel Jurassic succession on seismic section.

III) Pre-Jurassic 2: A horizon located inside the Triassic – Upper Paleozoic succession, and shows a subparallel reflection above a wedge-shaped geometry in the Horda Platform area on the seismic section.

IV) Top seismic basement: A horizon located at the base of the Triassic – Upper Paleozoic succession, which is displayed by the significantly wedge-shaped geometry under the Horda Platform, and shows a steeply declined reflection on seismic section.

Additional reflectors:

V) Postrift reference: A horizon located among the postrift successions above the BCU, and shows a subparallel reflection (Figure 1.2).

VI) Top Late Jurassic prerift: A horizon located at the top of the Late Jurassic prerift succession and beneath the BCU reflector.

The main reflectors were chosen in order to accomplish the objectives of this thesis work, namely, to map the three-dimensional architecture of an extensional fault system and to investigate their effect on the large-scale basin architecture. Therefore, the main reflectors were interpreted on every single selected seismic line (Figure 2.1 and Figure 2.2). On the other hand, additional reflectors were interpreted only on chosen lines. NVGT88-06 and NVGTI92-106 are reference seismic sections for the interpretation of the BCU, and NVGT88-05 is a reference seismic section for the three main reflectors beneath BCU because their seismic features are more pronounced and seismic quality is good. The interpretation started with the reference line (line L1 in Figure 2.3a), continued to the framework lines (line L1, L9, L5 and L6 marked as red dashed lines and framework lines in Figure 2.3a) and moved to all other selected lines (yellow lines marked as detailed line in Figure 2.3b) by using the same seismic characteristic/pattern from line to line.

Table 2.1 List of all selected lines for each interpreted reflector separately

Base Cretaceous Unconformity			Pre-Jurassic 1 & Pre-Jurassic 2 & Top seismic basement	Postrift reference & Top Late Jurassic pririft
NVGTI92-106	SH8001-L52	SH8401-L01W	NVGT88-05	NVGTI92-106
NVGTI92-108	SH8001-T56 ⁷	SH8401-L01E	NVGT88-06	NVGTI92-108
NVGTI92-109	SH8001-T59	SH8401-L04	NNST84-04	NVGTI92-109
NVGT88-05	SH8001-T67	SH8401-T07	NNST84-05	NVGT88-05
NVGT88-06	SH8001-T82	SH8401-T09S	SH8001-L05	NVGT88-06
NVGT88-07	SH8001-T83	SH8401-T09N	SH8001-L08	NVGT88-07
NVGT88-08	SH8001-T84	SH8401-T10S	SH8001-L10	NVGT88-08
NVGT88-09	MN9103-L03	SH8401-T10C	SH8001-L19	NVGT88-09
NVGT88-10	MN9103-L05	SH8401-T10N	SH8001-L23	NVGT88-10
NNST84-04	MN9103-L07S	SH8401-T11S	SH8001-L31W	NNST84-04
NNST84-05	MN9103-L07N	SH8401-T11N	SH8001-L35	NNST84-05
NNST84-06W ¹	MN9103-L09S	SH8401-T12	SH8001-L43	NNST84-06W
NNST84-07	MN9103-L09C	ST8201-L06	SH8001-T62 ⁸	NNST84-07
NNST84-09E ²	MN9103-L09N	ST8201-L08	SH8001-T65S	NNST84-09E
NNST84-09W	MN9103-L11S	ST8201-L10	SH8001-T65N ⁹	NNST84-09W
NNST84-10	MN9103-L11N	ST8201-L12	SH8001-T71S	NNST84-10
NNST84-11	MN9103-T02	ST8201-L13	SH8001-T71N	NNST84-11
NNST84-16S ³	MN9101-L01	ST8201-L15	SH8001-T82	NNST84-16S
NNST84-16C ⁴	MN9101-L02W	ST8201-L16	SH8001-T83	NNST84-16C
NNST84-16N ⁵	MN9101-L02CW	ST8201-L18	SH8001-T84	NNST84-16N
NNST84-17S	MN9101-L02CE	ST8201-L20	MN9103-L03	NNST84-17S
NNST84-17N	MN9101-L02E	ST8201-L28	MN9103-L05	NNST84-17N
NNST84-18S	MN9101-T03	ST8201-L31	MN9103-L07S	NNST84-18S
NNST84-18N	MN9101-T04	ST8201-L34	MN9103-L07N	NNST84-18N
SH8001-L08 ⁶	MN88-3-L07	ST8201-L36	MN9103-L09S	
SH8001-L19	MN88-3-T12S	ST8201-L38	MN9103-L09C	
SH8001-L23	MN88-3-T12N	ST8201-L40	MN9103-L09N	
SH8001-L31W	HRT91-T24	ST8201-L42	MN9103-L11S	
SH8001-L35	HRT93-T20	ST8201-L44	MN9103-L11N	
SH8001-L43	HRT93-T24		MN88-3-T11C	
SH8001-L51E			MN88-3-T11N	
SH8001-L51W				

Remarks:

1: W = West

6: L = Line

2: E = East

7: T = Trace

3: S = South

8: This line is used to interpret Top seismic basement only

4: C = Central

9: This line is not used to interpret Top seismic basement

5: N = North

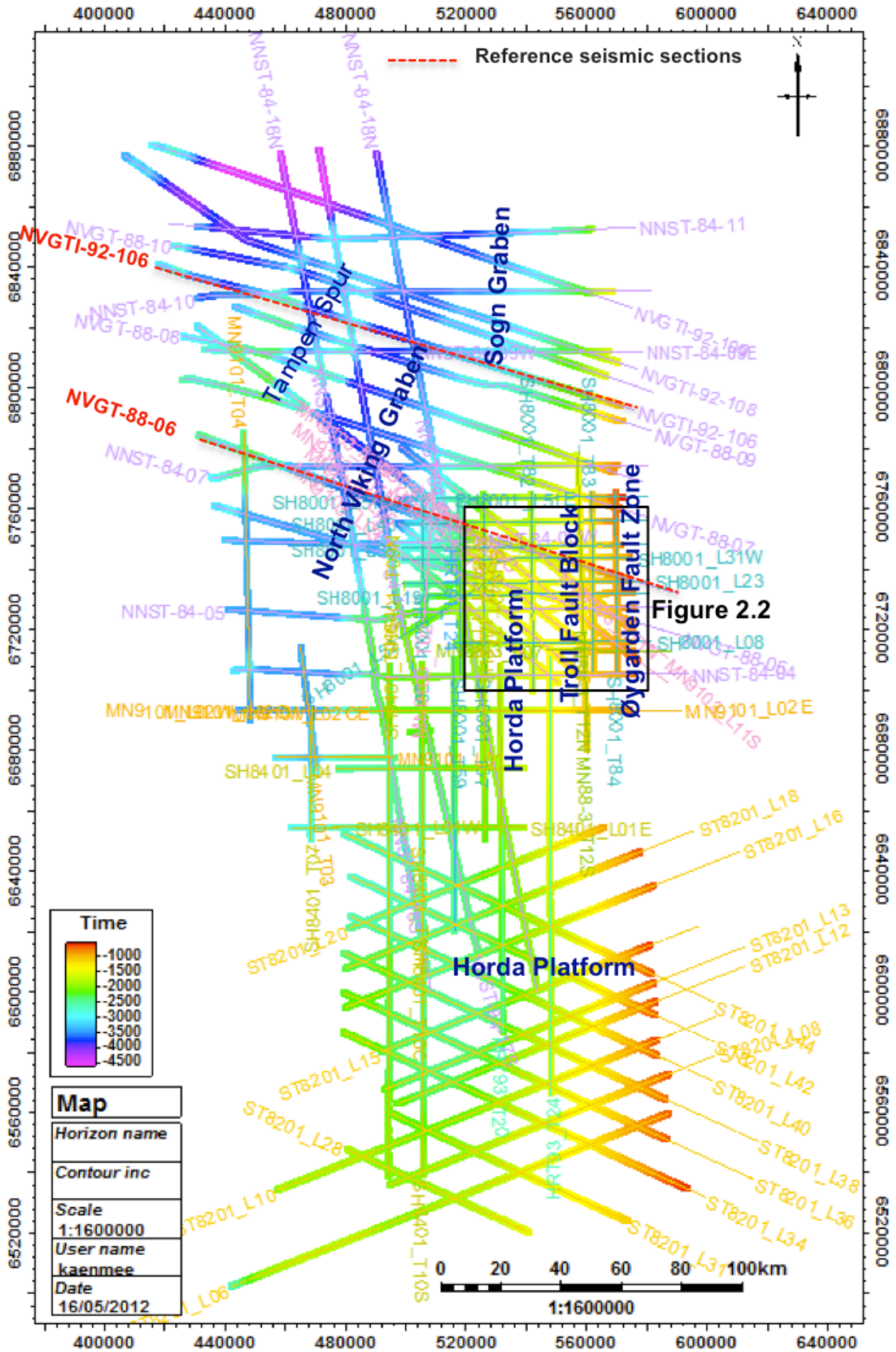


Figure 2.1 Selected 2D seismic lines for the interpretation of the BCU.

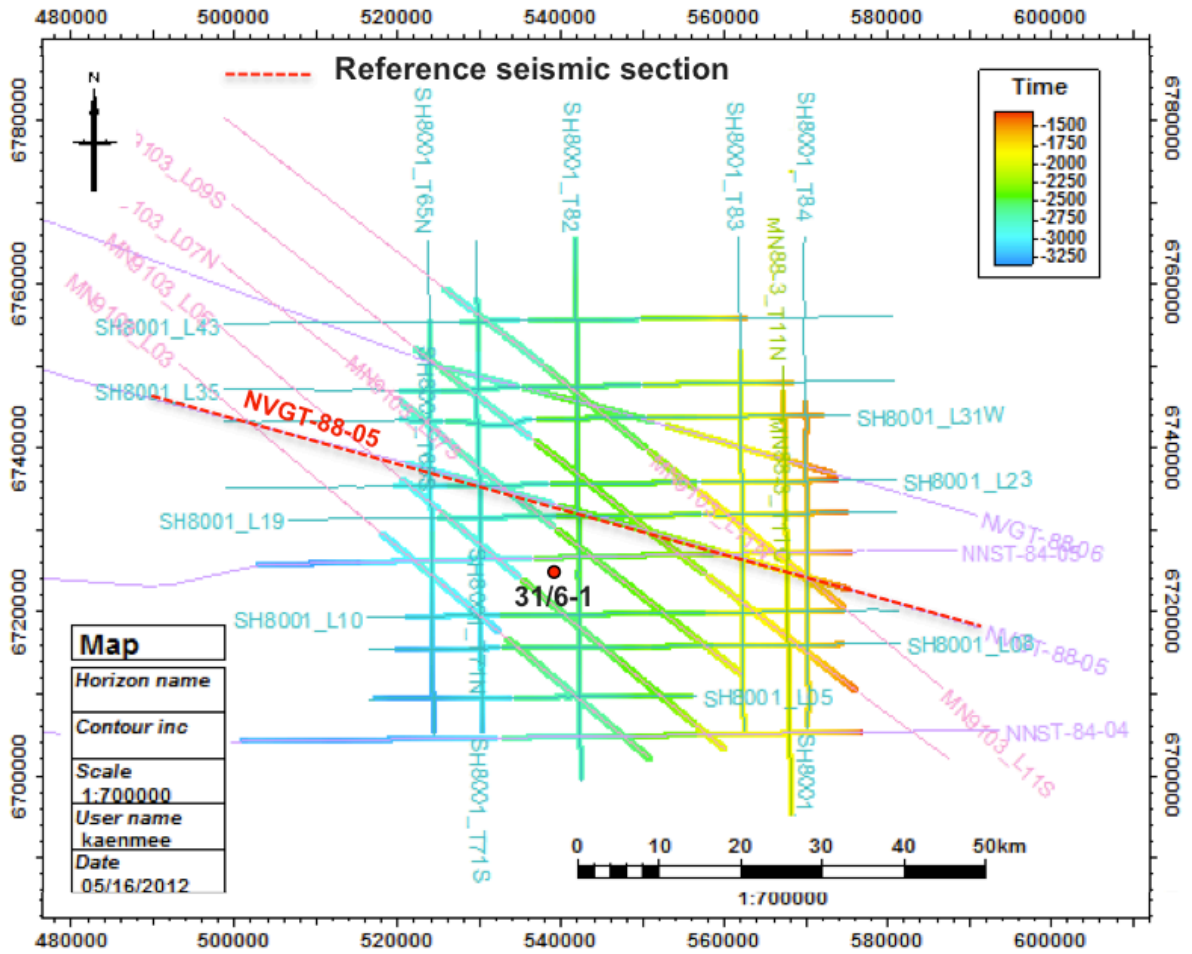


Figure 2.2 Selected 2D seismic lines for interpreting Pre-Jurassic 1, Pre-Jurassic 2 and Top seismic basement and location of well 31/6-1 penetrated these three reflectors on the Horda Platform.

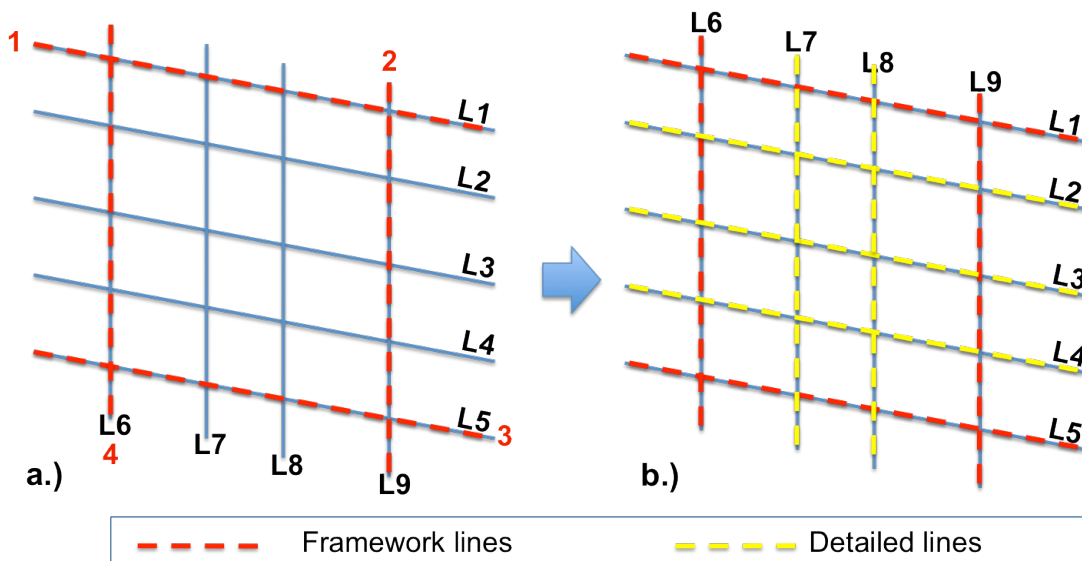


Figure 2.3 Example of the framework used for horizon interpretation. The interpretation would start from framework lines marked as red dashed lines: L1, L9, L5, L6 (in 2.3a) and would continue to the detailed lines marked as yellow dashed lines (2.3b).

Fault interpretation

Faults were interpreted as major when fault displacement was mapped as larger than 0.3 s TWT, whereas fault displacements smaller than 0.3s TWT were interpreted as indicative of second order faults. The same strategy was applied as above with the BCU, that is I started with the reference section to then move to the framework lines and the rest of the chosen lines (Table 2.1). When interpreting faults, I paid particular attention to:

- Termination of the same reflector on each side of a fault plane.
- A direct fault plane reflector produced by an acoustic impedance contrast across/within fault zone.
- A reflected fault plane from intersection line.

Fault polygons were then drawn manually on each time structural map for each horizon. Widths of the fault polygon were drawn accordingly to each fault displacement/ heave (Figure 2.4), by connecting foot- and hanging wall cutoff points.

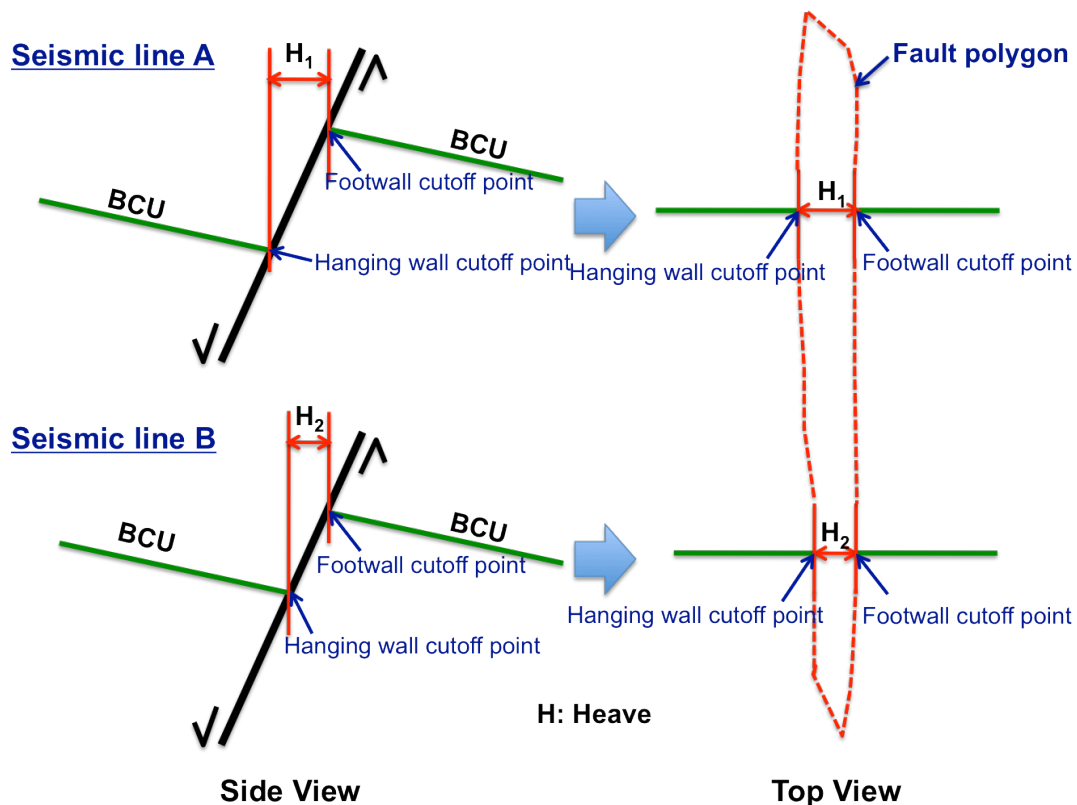


Figure 2.4 Example of fault polygon generation.

Structural time map

A structural time map is a contour map in time domain showing surface structures of one interpreted horizon and the fault interpretation associated to that reflector. One way to calibrate horizon and fault interpretations is to construct the structural time map of each horizon with the fault polygons on the map. The interpretation might not be logical if some abnormal features occur on the map. Hence, it is possible to check critical areas and re-interpret them to make their interpretation more robust.

3. Base Cretaceous Unconformity interpretation

The interpretation of BCU was done in order to map the large-scale basin architecture of the northern North Sea related to the extensional fault systems, and to find an interesting area for interpretations of the three deep reflectors beneath the BCU.

An unconformity represents a break in a stratigraphic record (Park, 1997). Three principal types of unconformity can be defined: 1) Disconformity, 2) Nonconformity and 3) Angular unconformity as given a simple explanation by in Figure 3.1. Disconformity is the term used to describe the hiatus at the boundary between two different sedimentary layers, for example, from carbonate to sandstone (Figure 3.1a). The term nonconformity, on the other hand, describes the boundary between igneous/metamorphic rocks and the overlying sedimentary rock (Figure 3.1b). Angular unconformity refers to a hiatus between two differently oriented sedimentary successions (Figure 3.1c). The BCU can be any of the three types depending on where it is observed in the North Sea. The variations in each type of unconformity reflect mainly different structural positions within the basin (Kyrkjebø et al., 2004) as shown in figure 1.10.

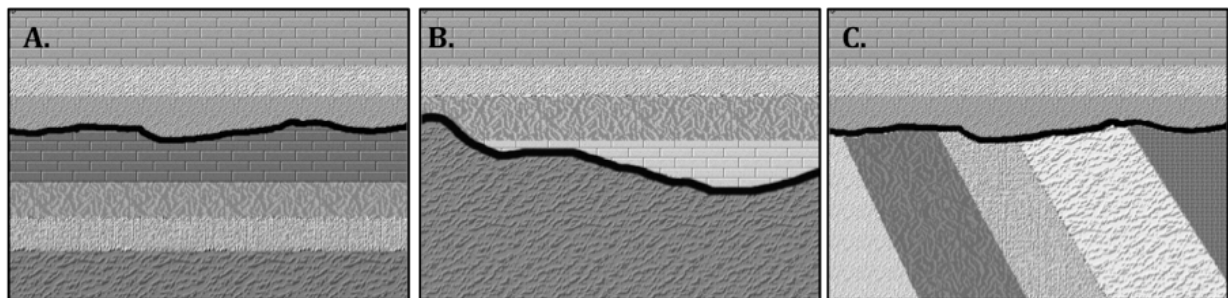


Figure 3.1 Simple sketches of unconformity. A.) Disconformity, B.) Nonconformity and C.) Angular unconformity¹.

Even though Lower Cretaceous sediments do not always overlay this unconformity (Kyrkjebø et al., 2004), the term “Base Cretaceous Unconformity” will be used in this thesis because all the processes that created the BCU were connected to the Jurassic-Cretaceous syn- or post-rift transition in the northern North Sea. Moreover, the unconformity resulted from several processes of both regional and local significance; therefore, this overview term is used to simplify. This unconformity is also frequently known as “late Cimmerian unconformity” used by many workers (e.g. Heybroek et al. 1967; Hallam 1971; Ziegler 1990), and “northern North Sea Unconformity Complex” suggested by Kyrkjebø et al. (2004). However, these terms are used to refer to both local and regional unconformities during the latest Jurassic-early Cretaceous period covering most of the basins in the North Sea (Kyrkjebø et al., 2004).

3.1 Seismic interpretation

The interpretation of the BCU is based on the characteristics listed below:

- A strong reflector representing an abrupt change in facies resulting in distinct reflection due to high impedance contrast.
- A termination/ending point of fault symbolizing a change in tectonic style between the heavily faulted upper Jurassic (synrift) and the unfaulted Cretaceous (post-rift) sequences.
- A boundary between postrift sequences, the relatively constant-thick stratigraphic layers above the unconformity due to a continuous postrift sedimentation and stage of no tectonic events, and the synrift sequences, displayed a wedge-shaped geometry overlying the constant-thick layers of prerift sediment.

In this thesis, one method used to correlate and calibrate the BCU is to check a thickness of the postrift reference above major unconformity across the subdomain configurations within the basin. Ideally, the thicknesses of postrift succession from different locations within the basin are supposed to be likely the same due to constant subsidence rate and no tectonic events affecting the sedimentation during this period. The Petrel tool “flatten horizon” has been used here to visualize the geometry of underlying beds and structures at the time of deposition of the stratigraphic level of the Late Jurassic reference postrift reflector (light blue line) as shown in Figure 3.2a at the time of depositions (Figure 3.2b). This type of analysis allows for an easier interpretation of a chosen reflector (e.g. the BCU) across the rotated fault block areas and to other structural subdomains. Namely, after flattening the reference horizon the thicknesses of postrift can be measured to locate BCU across the sub-platforms areas. Additionally, in the example of Figure 3.2 the "Top Late Jurassic prerift" reflector (yellow line) is identified using the characteristics of the prerift and the postrift sequences as mentioned earlier.

Kyrkjebø et al. (2004) stated that several factors affected the complexity of the unconformity in the northern North Sea, including the general basin geometry, the position within the basin, the overall basin-scale fault configuration, possible fault-related variations in subsidence pattern, and possible spatial and temporal heat flow variations. Therefore, the BCU interpretation has been done in this thesis in order to familiarize with obvious seismic interpretation tools and techniques, seismic patterns and characteristics, and to derive the big picture of the complex structural framework of the northern North Sea basin. The following sections will be elaborating on each of the structural/morphological features separately with regard to the BCU interpretation according to the configuration classification presented in Figure 1.10 and the reference seismic section NVGT88-06 (Figure 3.3).

Platforms

The Øygarden Fault Zone, the Troll Fault Block and the Horda Platform are located at the platform region. Regarding the observations and the Figure 1.10, the common types of unconformity found at the platforms are varied from the flat angular unconformity, the faulted unconformity, the merging unconformity and the eroded fault block unconformity. Examples of each type are visible clearly from reference seismic section from line NVGT88-06 (Figure 3.3) and detailed interpretation in Figure 3.4 to 3.8.

According to the reference seismic section, NVGT88-06 in Figure 3.3, the three significant reflectors are present underneath the BCU on the Horda Platform, the Øygarden Fault Zone and the Troll Fault Block. Therefore, this area is interpreted thoroughly with more seismic lines than the rest of the study area.

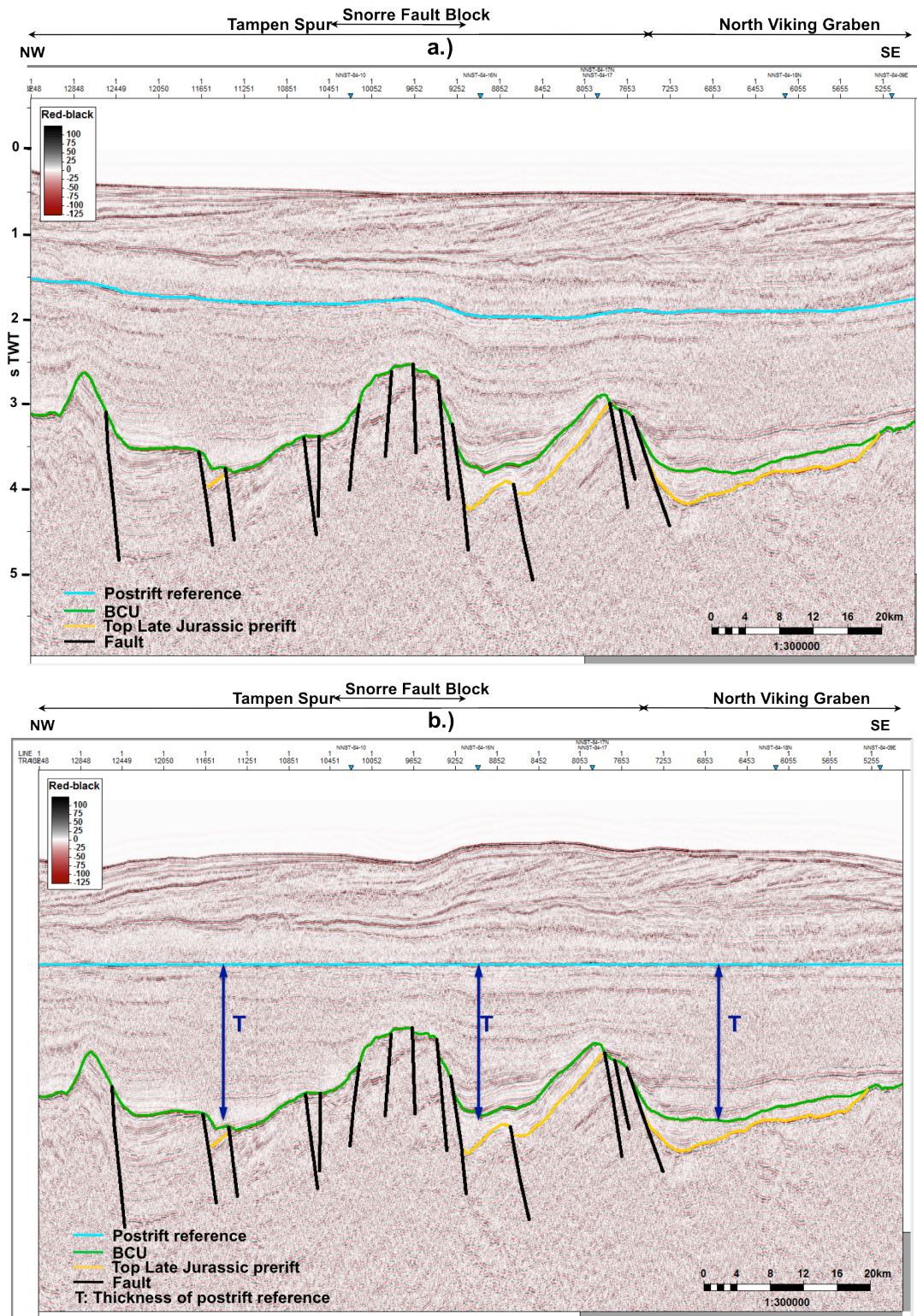


Figure 3.2 Illustration of the concept built in the “Flatten horizon” tool to locate the BCU across rotated fault blocks along the 2D seismic line NVGTI92-106: a.) Before and b.) After the flattening the postrift reference reflector. This tool helps to locate the BCU reflector more easily (the flattened horizon has been subjected to differential compaction, so that the layers beneath will thus be changed accordingly).

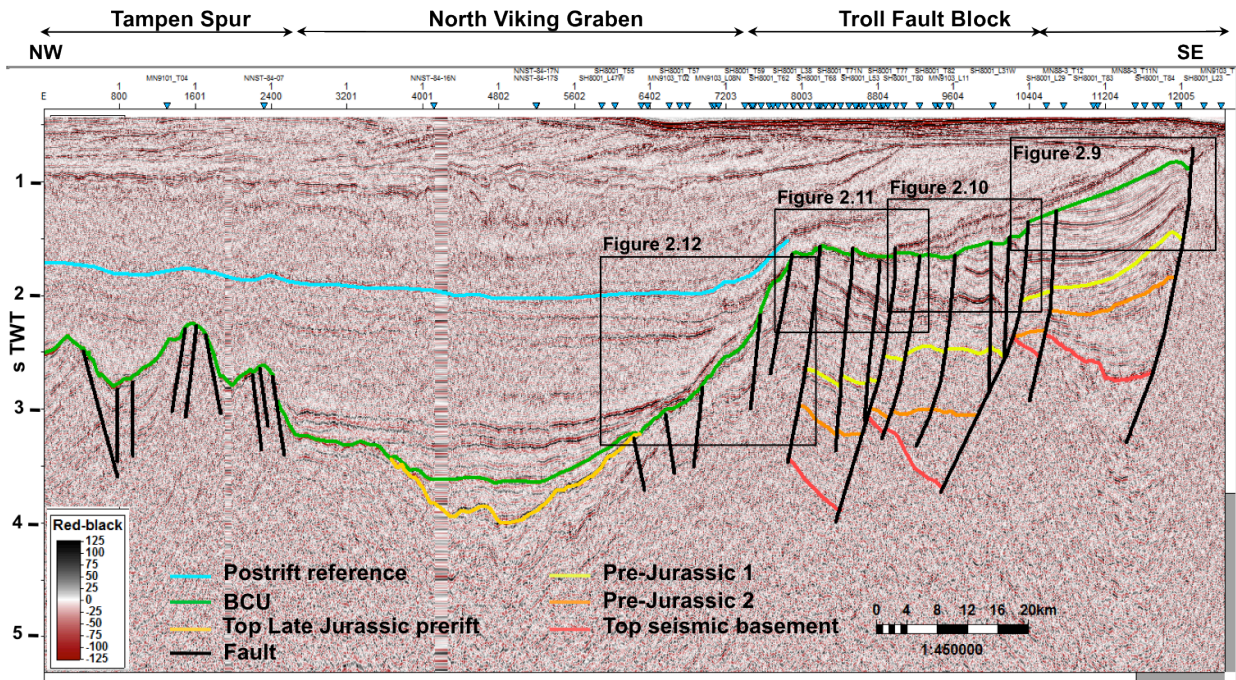


Figure 3.3 NVGT88-06 reference seismic section for Base Cretaceous Unconformity

The angular unconformity is mostly pronounced and visible on a regional scale over the Troll Fault Block and the Øygarden Fault Zone (Figure 3.4) but it is observed as a disconformity on the Horda Platform and in the northern Troll Field (Figure 3.8), indicating the variations of the complex unconformity across the structural locations.

Apparently, a merging of unconformities occurred at the proximal parts of the platforms. An underneath unconformity united with the post-glacial Pliocene–Pleistocene unconformity and combined them into one unconformity (Figure 3.6). Hence, the unconformity consists of several erosional surfaces, which are related to both local and regional vertical movements of the subsurface as well as changes in sea level.

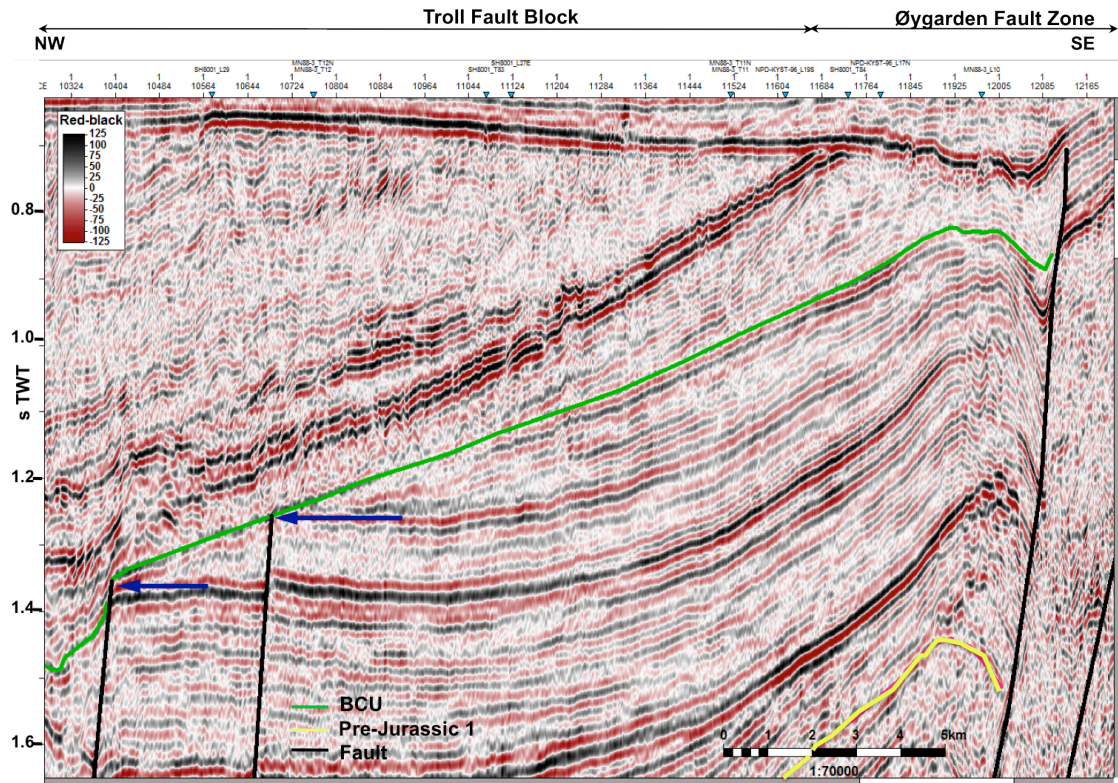


Figure 3.4 Illustration of the flat angular unconformity from 2D seismic line NVGT88-06. It is characterized by downlap from above and top-lap from beneath the unconformity reflector. Locally, and close to marginal horst, the angular unconformity is commonly more clearly seen.

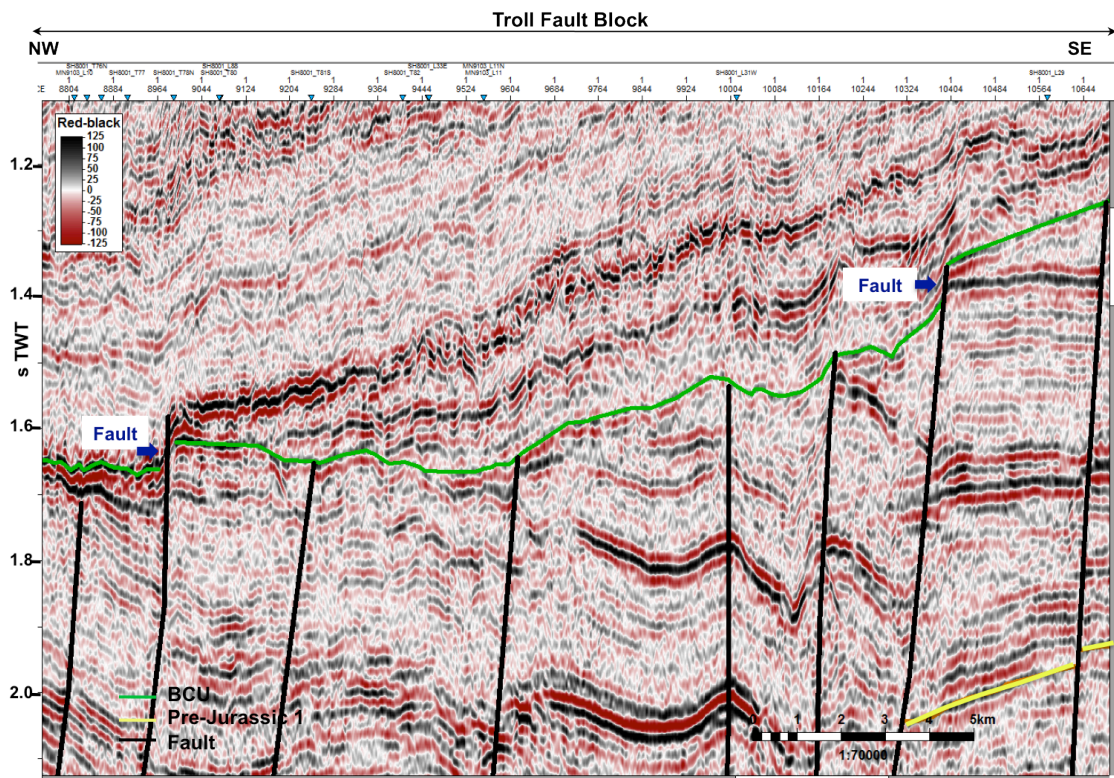


Figure 3.5 Illustration of the faulted unconformity from 2D seismic line NVGT88-06. A discontinuous reflector characterizes the faulted unconformity across the fault planes.

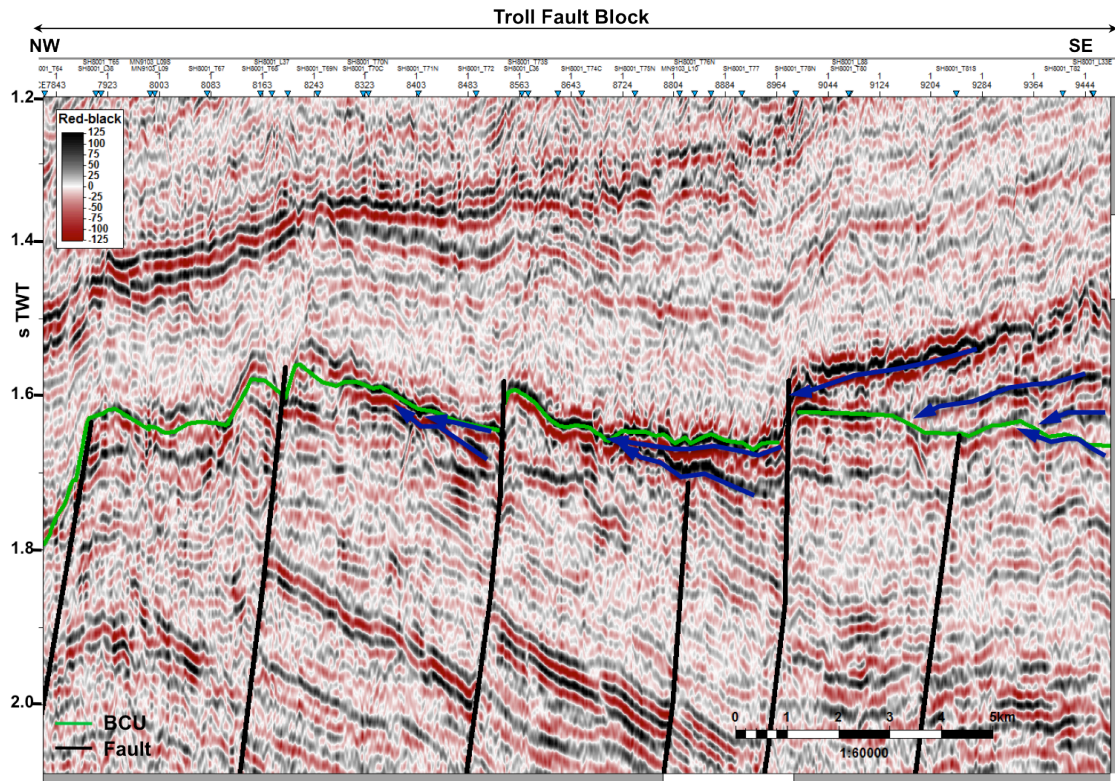


Figure 3.6 Illustration of the merging unconformity from 2D seismic line NVGT88-06. This merging unconformity is marked by truncation of the strata below and onlap of the strata above it.

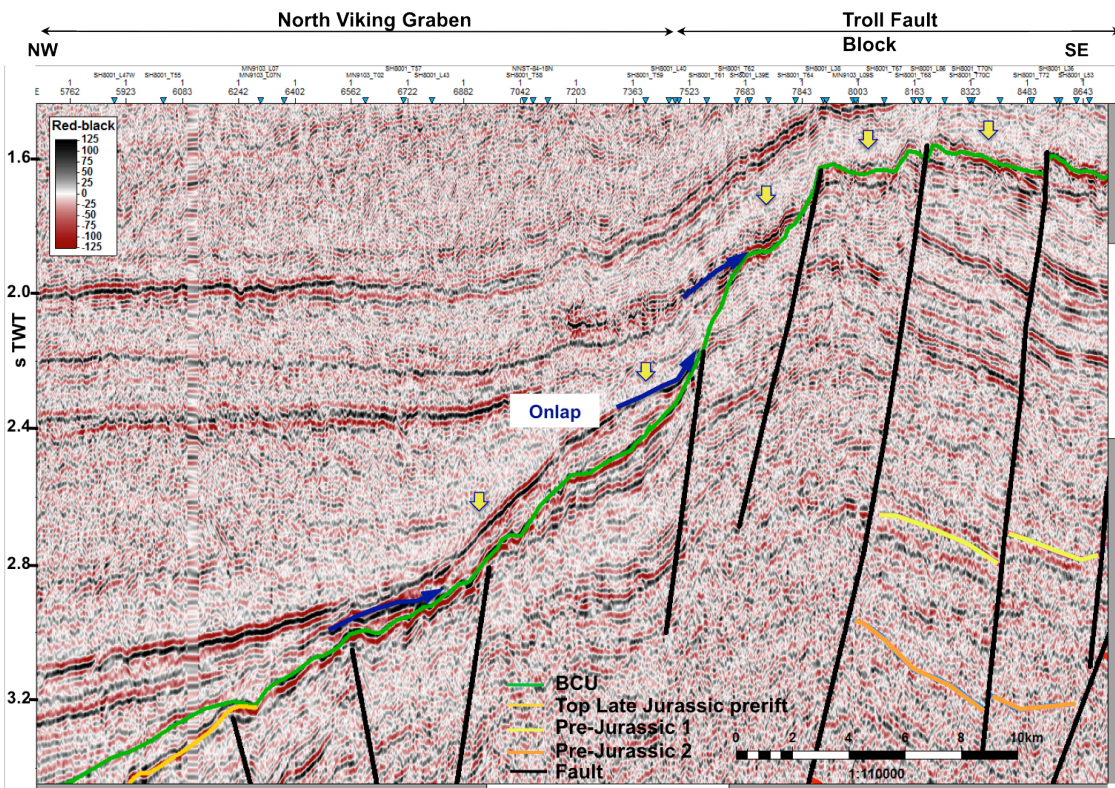


Figure 3.7 Illustration of the eroded fault block sequence, indicated by yellow arrows, from the 2D seismic line NVGT88-06. This unconformity is commonly found at the elevated areas such as the basin flank or sub-platforms, and displayed as a strong reflector. Onlap surfaces are also visible here at the center of the figure.

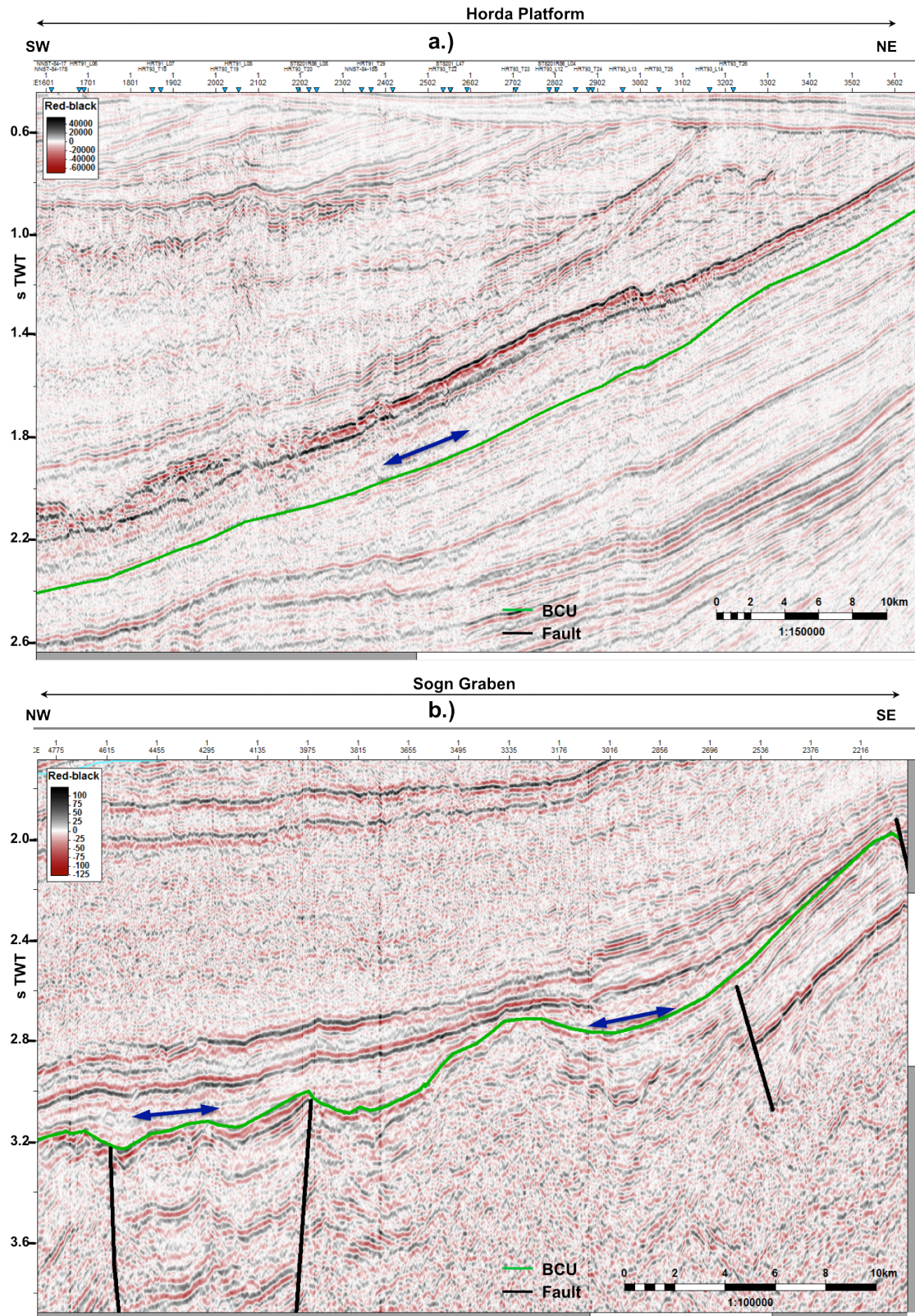


Figure 3.8 Illustrations of the disconformity. a.) Configuration in the area of the Horda Platform from 2D seismic line ST8201-L20. The disconformity is characterized by relatively parallel strata below and above the unconformity. Hence, the Horda Platform fundamentally remained a stable part of the rift system also during the post-rift development. In other words, a constant subsidence took place but less fault block rotations. b.) Disconformity in the northern Troll field from 2D seismic line NVGTI-92-106.

Interior graben

The Sogn Graben and the North Viking Graben are examples of the interior graben in the study area. Both grabens are axially oriented northeast-southwest. The deepest part of the basin corresponds to its axial portion and is characterized by less intense faulting, which leads to a simpler structural configuration than that at the margins. A possible explanation for less pronounced impedance contrast, weak reflector, in the basin parts is because of a stage of minimum surface erosion and the unconformity corresponds to a minor facies change between conformable sequences. The Disconformities are frequently found in these locations, together with the occurrence of seismic features such as onlap, downlap and toplap (Kyrkjebø et al., 2004). However, faulted unconformity is also identified along the bounding faults to the rotated fault block area (Figure 3.9) as a typical unconformity character in the sub-platform area.

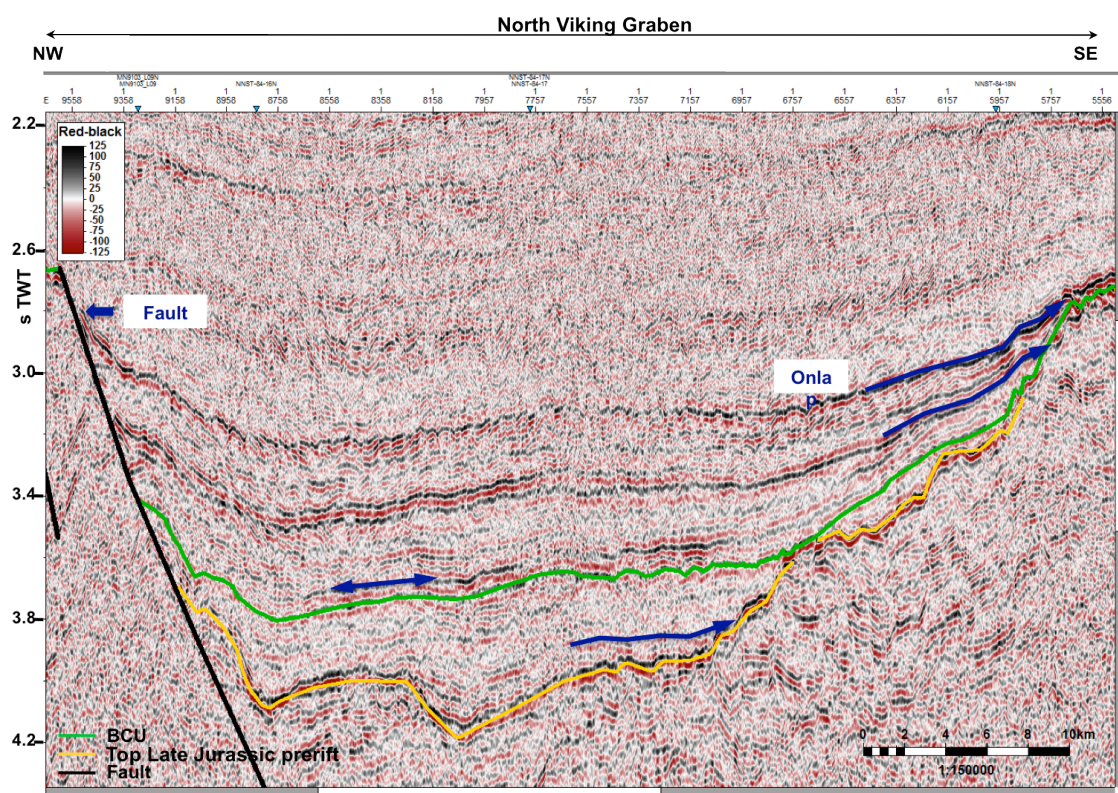


Figure 3.9 Illustration of the disconformity (indicated by a double arrow), faulted unconformity on the left side of the figure along the bounded fault to the rotated fault block area, and onlap features from a graben area as seen in the 2D seismic line NVGT88-07. The disconformity is displayed above the wedge-shaped geometry of synrift sequence, an area from a yellow line to a green line. The onlap features are clearly seen in both postrift and synrift sequences.

Sub-platforms and rotated fault blocks

In the study area, the Tampen Spur and the Snorre Fault Block, situated at the transition between the East Shetland Platform to the east and the North Viking Graben to the west (Figure 1.2), correspond to sub-platforms associated with rotated fault blocks. Kyrkjebø et al. (2004) mentioned that the occurrence of rotated fault blocks below the BCU unconformity is more common in the northern than in the southern Viking Graben. Faulting in the Sogn Graben and at the transition to the Møre Basin has been considered to have caused the rotations of the strata at

the Tampen Spur and the Snorre Fault Block, and lately the crests of the unstable fault blocks were eroded to be smooth surfaces.

Pronounced unconformities in this area are the flat angular unconformity (Figure 3.10), the faulted unconformity and the eroded fault block crests (Figure 3.11).

At the intrabasinal block located between the Tampen Spur and the Snorre Fault block, the unconformity consists of several separate unconformity surfaces that merge into one in the footwalls of rotated fault blocks (Figure 3.11). Kyrkjebø et al. (2004) stated that an interpretation of wire line logs from the Moray Firth, the Ling Graben and the area south of the Egersund Basin by Rawson & Riley (1982) supported the existence of the merging unconformity by establishing no fewer than 13 unconformity surfaces merged into one at the crest of the rotated fault blocks.

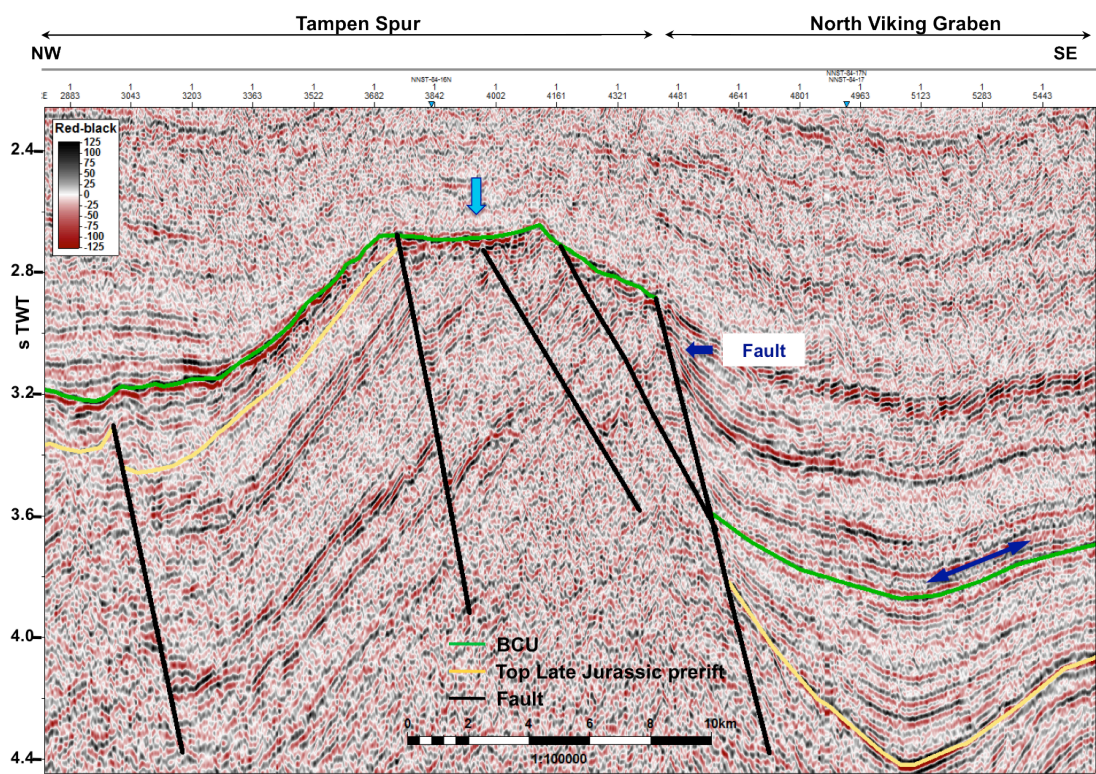


Figure 3.10 Illustration of the flat angular unconformity (indicated by a light blue arrow) from the 2D seismic line NVGT88-08, showing complex erosional patterns superimposed on the unconformity.

3.2 Complexity of the Base Cretaceous Unconformity

The changes in the characteristics of the BCU have been noticed locally and regionally across the study area, depending strongly on structural and geographical position within the basin. The character of the unconformity varies among the locations in the north: the Tampen Spur and the Snorre Fault Block, the North Viking Graben, the Sogn Graben (Figure 3.12a & 3.12b), and locations in the central part: the Troll Fault Block, the Øygarden Fault Zone (Figure 3.12c), and locations in the south: the Central Viking Graben and the Horda Platform (Figure 3.12d). The occurrence of the BCU is significantly different, namely, at the platform area, for example, disconformity is displayed in the north, transferred to angular-, faulted and eroded unconformity in the central, and changed to disconformity again in the south (Figure 3.2). These

differences in character of the BCU can possibly be influenced by the slightly difference in tectonic activities along the area as the Jurassic-Cretaceous rifting is believed to start earlier in the south and the effects of another rifting in the Møre Basin in the north (Zanella and Coward, 2003).

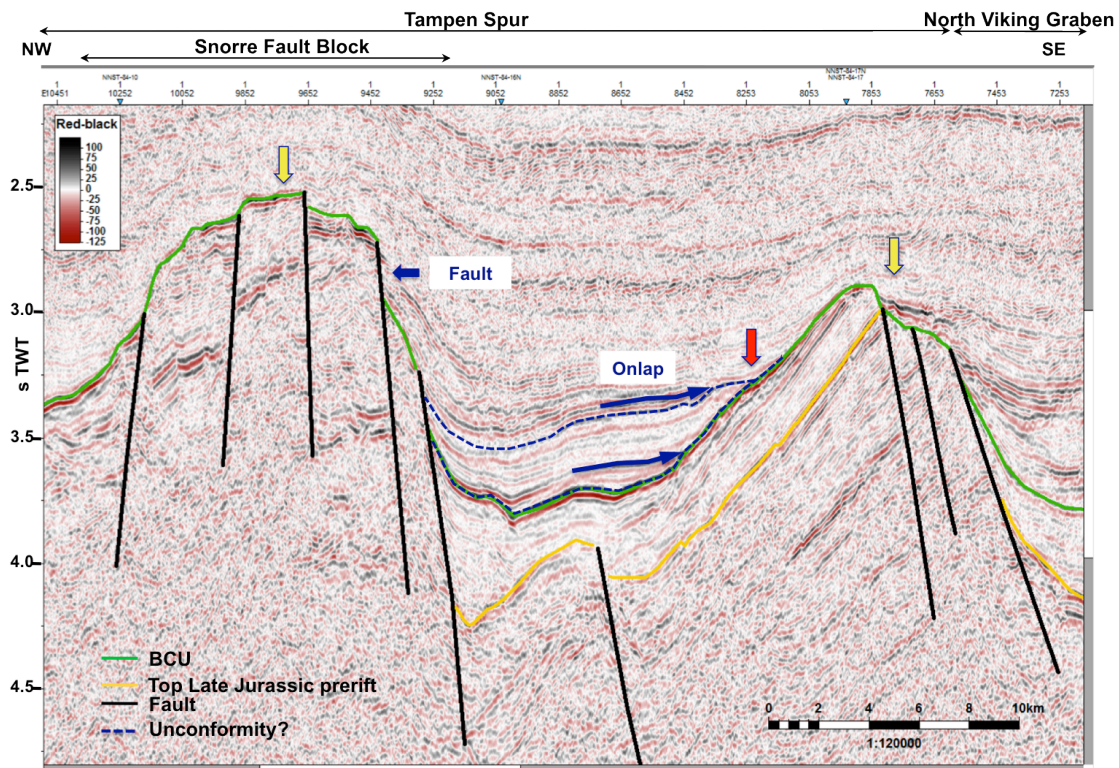


Figure 3.11 Illustrations of the faulted BCU and the eroded fault block crests (indicated by yellow arrows) from the 2D seismic line NVGTI92-106. The unconformities are commonly identified at the sub-platforms associated with the onlap features in the interior grabens located in between the crests. The curvature of the onlap surface and the angle of onlap vary as a function of the position along the interior graben axis. A red arrow indicates possible merging unconformity.

Kyrkjebø et al. (2004) mentioned that the poorly understood uplift, which took place in the area from the Permo-Triassic rift to the present day, might have contributed to the complexity of this unconformity (It should be noted that Kyrkjebø et al. (2004) used the term ‘northern North Sea Unconformity Complex’ instead of BCU). Besides, significant erosion occurred on the high-elevated areas, such as the platform and sub-platforms, may have affected the occurrence of the BCU locally and regionally. In addition, the effects from fault-block rotation, changing sea level, gravity instability and varying sediment input might complicate the complexity of the BCU along the interior grabens.

3.3 Mapping

The final structural time map of the BCU was constructed by interpreting the sections listed in Table 2.1 and shown in Figure 3.13. The warm colors on the map represent higher elevations; in contrast, cool colors symbolize lower elevations, and fault polygons are exhibited by grey color. The depressed elongated troughs, the North and Central Viking Grabens, are located at the central part and bounded by parallel faults and elevated shoulders, the Snorre Fault block and the Troll fault block. The BCU’s structures are associated with normal faults strongly

dipping toward the deepest part of the basin clearly show the classic architecture of extensional rift basin.

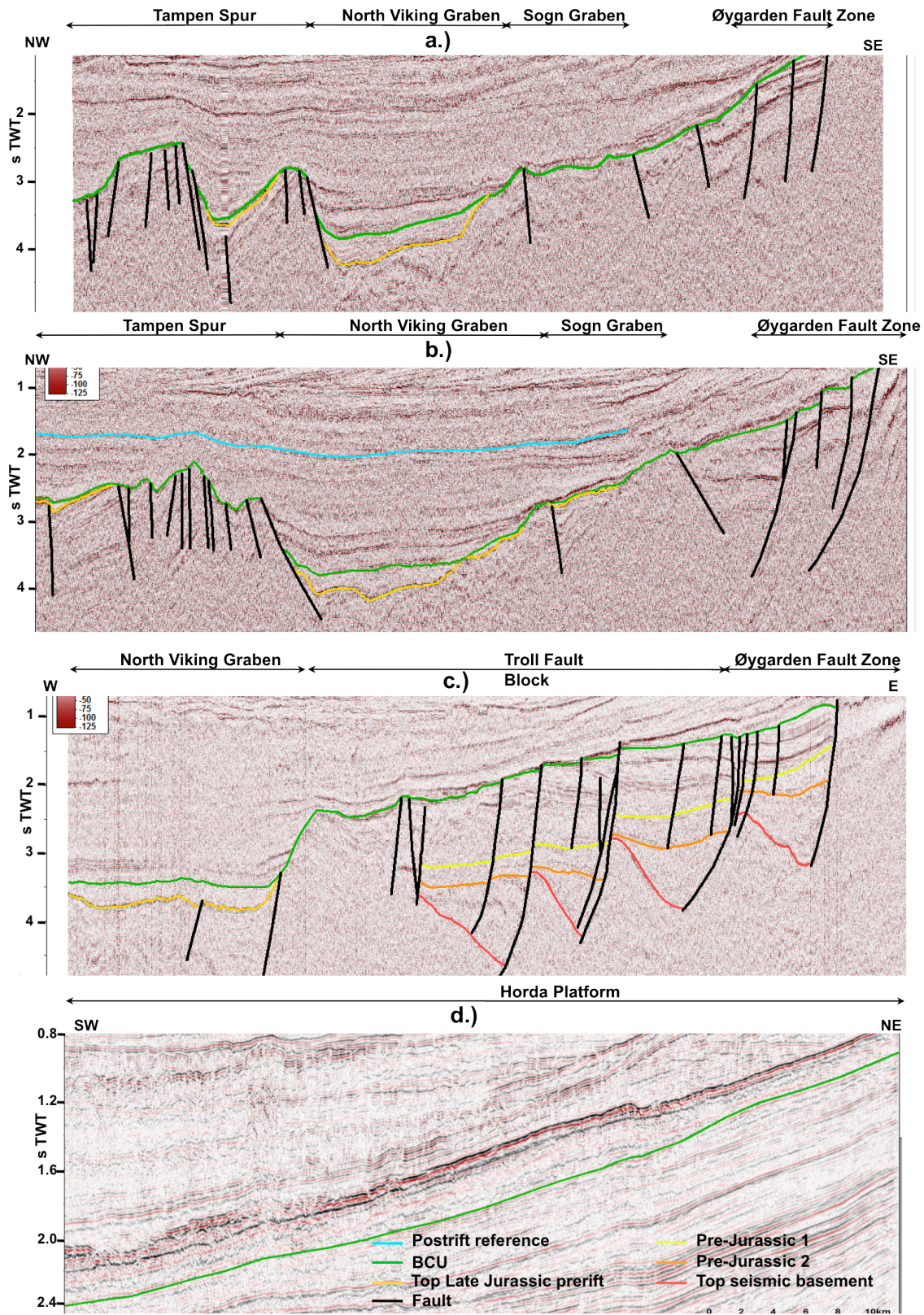


Figure 3.12 Examples of the complexity of the BCU. a.) Seismic section from 2D seismic line NVGT88-09 in the north study area, b.) Seismic section from 2D seismic line NVGT88-07 in the north study area, c.) Seismic section from 2D seismic line NNST84-05 in the central, d.) Seismic section from 2D seismic line ST8201-L20 in the south.

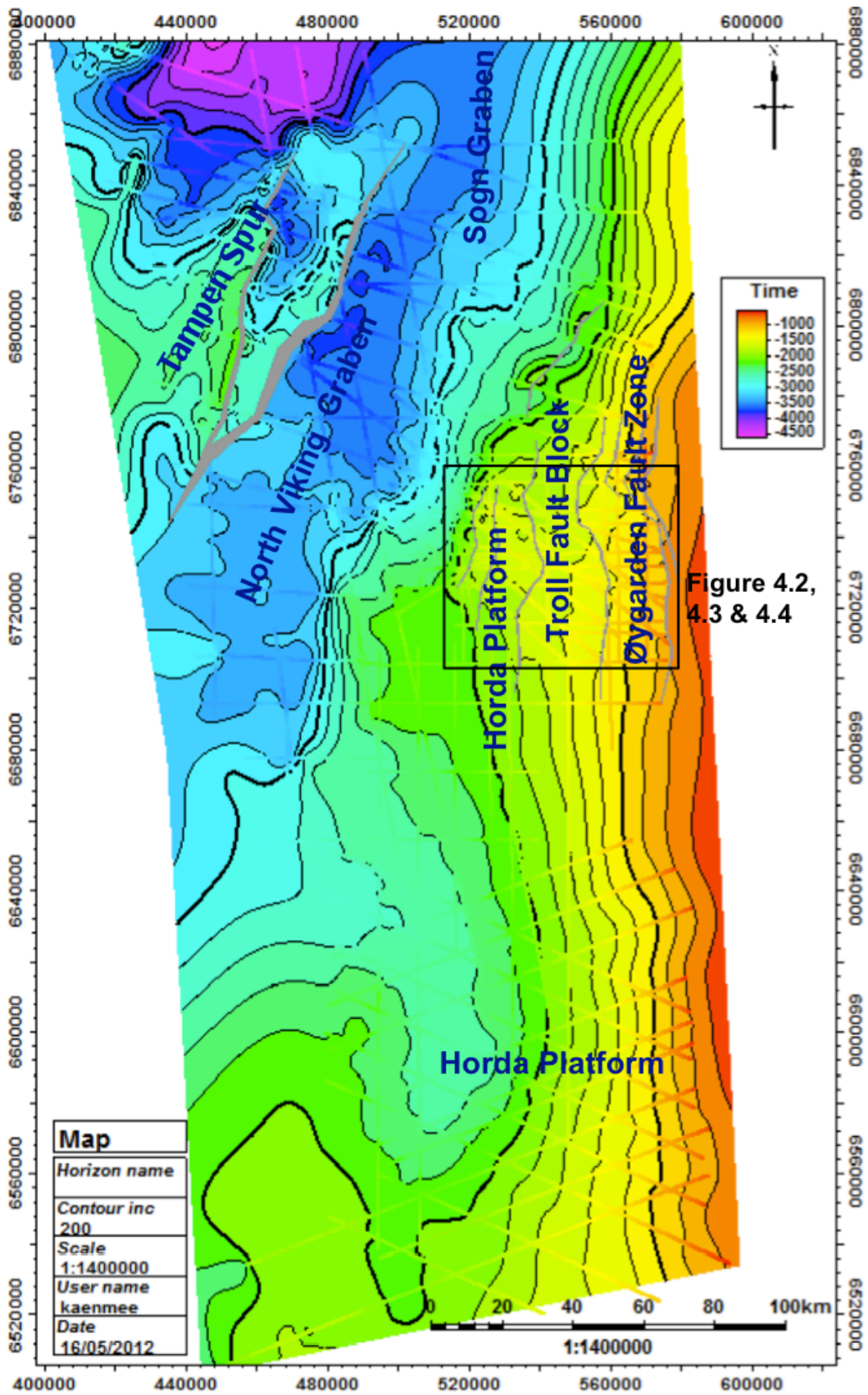


Figure 4.2, 4.3 & 4.4

Figure 3.13 Structural time map of Base Cretaceous Unconformity

4. Deep reflector interpretation

In order to investigate in detail the displacement gradients and linkage of the fault system under the Horda Platform, and to comprehend stratigraphy and sedimentary architectures related to rift basin development, thus, three deep pronounced reflectors: Pre-Jurassic 1, Pre-Jurassic 2 and Top seismic basement, underneath the BCU under the Horda Platform and the Øygarden Fault Zone, were chosen to interpret (Figure 4.1). The following sections will be elaborating on each reflector separately with regard to the reference seismic section NVGT88-05 (Figure 4.1). An interesting area to interpret all three reflectors below the BCU is displayed in Figure 3.13, and the chosen interpreted lines for these three reflectors are in Table 2.1 and Figure 2.2.

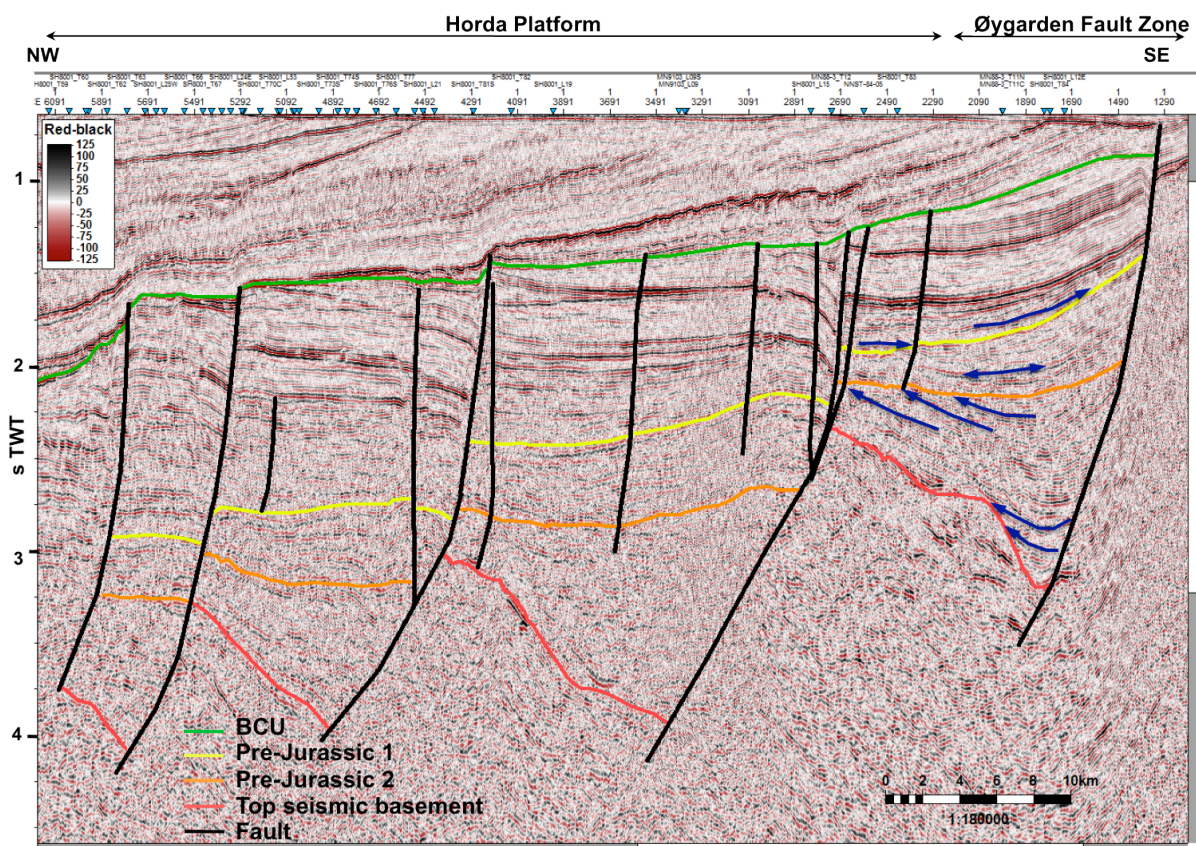


Figure 4.1 Illustration of interpretation of faults and seismic horizons in the Horda Platform area from the reference 2D seismic line NVGT88-05.

4.1 Pre-Jurassic 1

4.1.1 Seismic interpretation

The Pre-Jurassic 1 reflector is characterized by a likely first declined reflector beneath a group of strong seismic reflectors underneath the BCU (Figure 4.1). In this thesis, the term “Pre-Jurassic 1” is used to refer to the top of the Permo-Triassic succession (i.e. the base of the Jurassic) at the top of wedge-shaped sedimentary packages believed to having been deposited before the Late Jurassic rifting. Additionally, Zanella and Coward (2003) and Christiansson et al.

(2000) established that the top of the Jurassic succession is largely identified by the BCU in the Horda Platform area (Figure 1.2 and 4.1). Hence, the term “Pre-Jurassic 1” is applied to the reflector situated at the top of a group of steeper strata underneath the “Top Jurassic”, identified by Zanella and Coward (2003) and Christiansson et al. (2000), as shown by the yellow line in Figure 4.1.

4.1.2 Mapping

The structural time map of the Pre-Jurassic 1 is shown in Figure 4.2. According to Figure 4.2, a large amount of fault traces are starting to show up on this map compared to the structural time map of the BCU (Figure 3.13). This implies the different stages of basin development, namely, faulted succession in the synrift stage or higher magnitude of tectonic activity, in contrast, and unfaulted sequences in the postift stage or with lower magnitude of tectonic activity. Moreover, these fault traces are relatively narrow compared to the fault polygons in the following maps from the deeper reflectors. This is related to the increasing heaves recorded by the faults at depth. This observation indicates that the amount of extension in the pre-Jurassic rift phases were larger than the Jurassic extension (as argued also by Christiansson et al.).

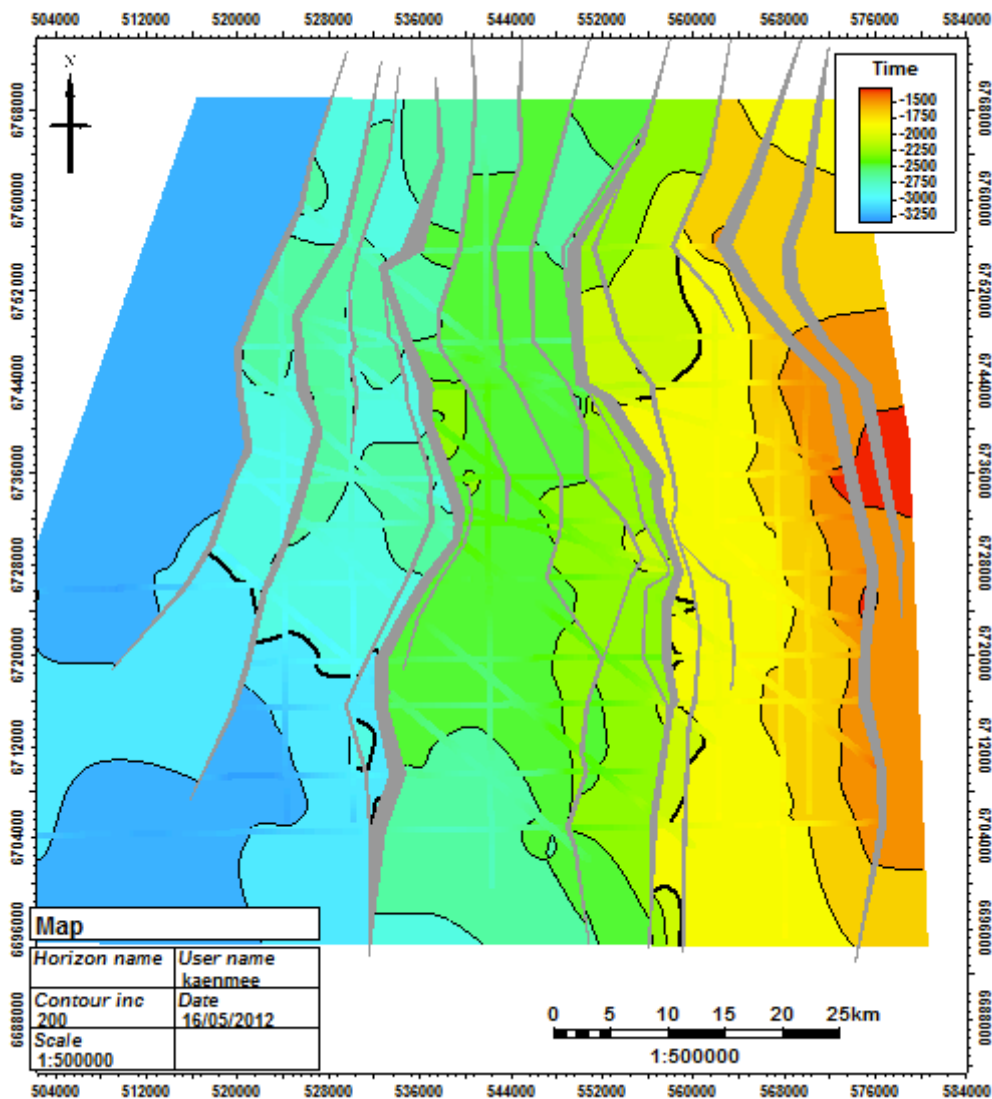


Figure 4.2 Structural time map of the Pre-Jurassic 1.

4.2 Pre-Jurassic 2

4.2.1 Seismic interpretation

In this thesis the term “Pre-Jurassic 2” is used to refer to the lowermost flat reflector beneath the Pre-Jurassic 1 reflector located at the top of large wedge-shaped bodies above the seismic basements (Figure 4.1) on the Horda Platform. This synrift wedge formed either before or during the Permo-Triassic rifting. According to Zanella and Coward (2003) and Christiansson et al. (2000), this seismic reflector is of Upper Paleozoic to Triassic age. The selected interpreted lines are already shown in Table 2.1 and Figure 2.2.

4.2.2 Mapping

The structural time map of Pre-Jurassic 2 is shown in Figure 4.3. The larger fault polygons are clearly seen on this map compared to the map of the Pre-Jurassic 1 in the previous map (Figure 4.2). This implies the larger heaves recorded at depth as mentioned before. In addition, the relationship between the faults and the topography of the faulted surface are better seen on this map (Figure 4.3). That is, slightly higher areas in the central part of the footwalls indicate the centers of the footwall uplift, and slightly depressed areas displayed on the hanging walls at the opposite location indicate the subsidence.

4.3 Top seismic basement

4.3.1 Seismic interpretation

The structural framework of basin development in the North Sea is well documented (e.g. Christiansson et al. (2000), Kyrkjebø et al. (2004), Lister et al. (1991)). The detailed interpretation of the seismic basement, on the other hand, is not as straightforward because of the less resolution of seismic reflection data comparatively to the shallower sections or the lack of strata-age identifications correlated from well data. In this thesis the term “Top seismic basement” is used to refer to the strongly inclined reflectors against which onlap features are clearly seen to terminate and it continued upward to the Pre-Jurassic 2, and this pronounced reflector is also situated at the base of the massive wedge geometry (Figure 4.1). One deep well, well 31/6-1 was recorded to drill into crystalline basement on the Horda Platform and basement surface is well correlated to the strong reflector on seismic section (Christiansson et al., 2000). Note that this “Top seismic basement” reflector is not necessarily the top of the crystalline basement. However, This reflector can be traced further onto the Horda Platform but not in center of the Viking Graben due to poorer seismic resolution at depth. The used seismic lines are shown in Table 2.1 and Figure 2.2.

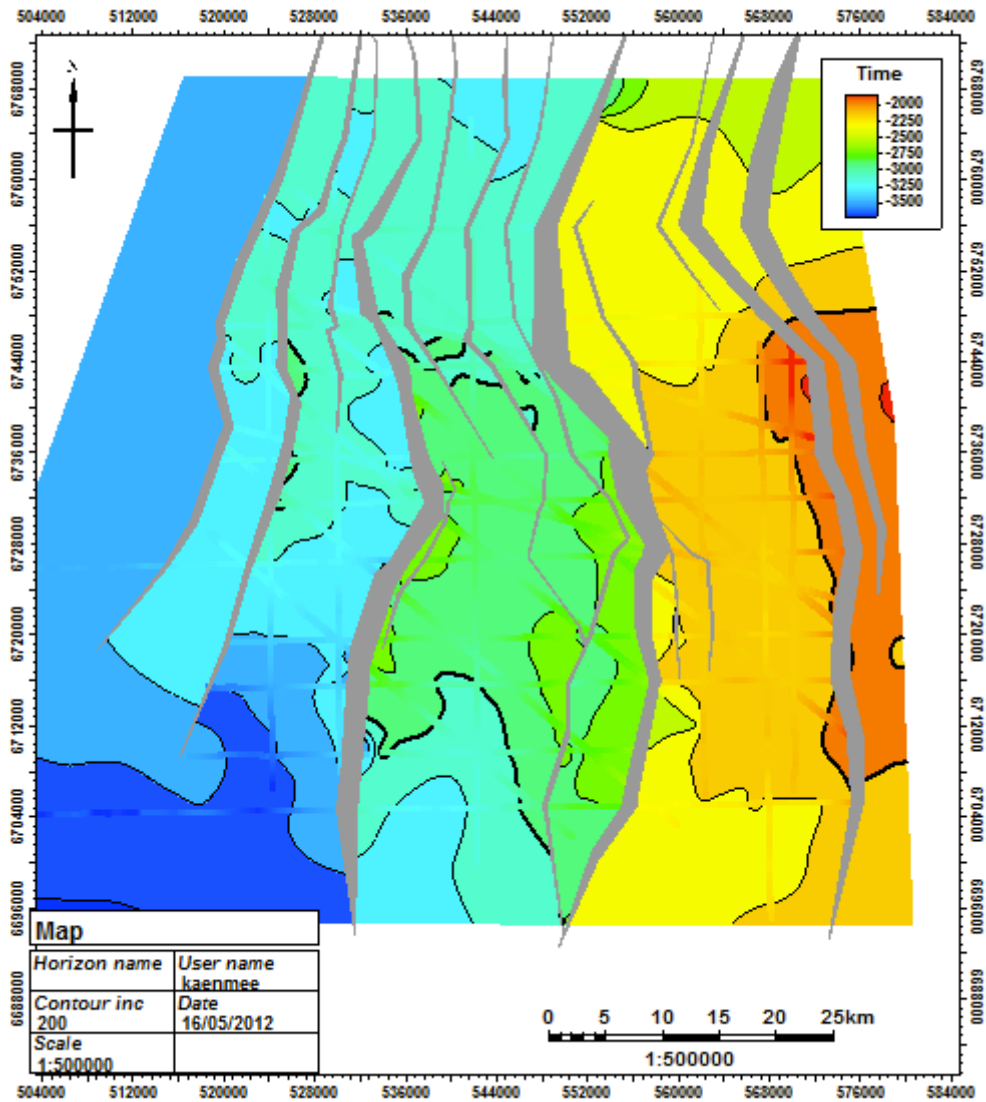


Figure 4.3 Structural time map of the Pre-Jurassic 2

4.3.2 Mapping

The structural time map of Top seismic basement is shown in Figure 4.4. On this map, the fault polygons are much wider than in the preceding maps. The variations in horizon topography along the fault planes are most pronounced here, namely, the highest elevated area and deepest depressed area are shown mostly in the central part of each fault. The larger fault polygons display larger significant differences in surface topography between the footwall and hanging wall topography than smaller fault polygons in the previous two maps from the shallower positions.

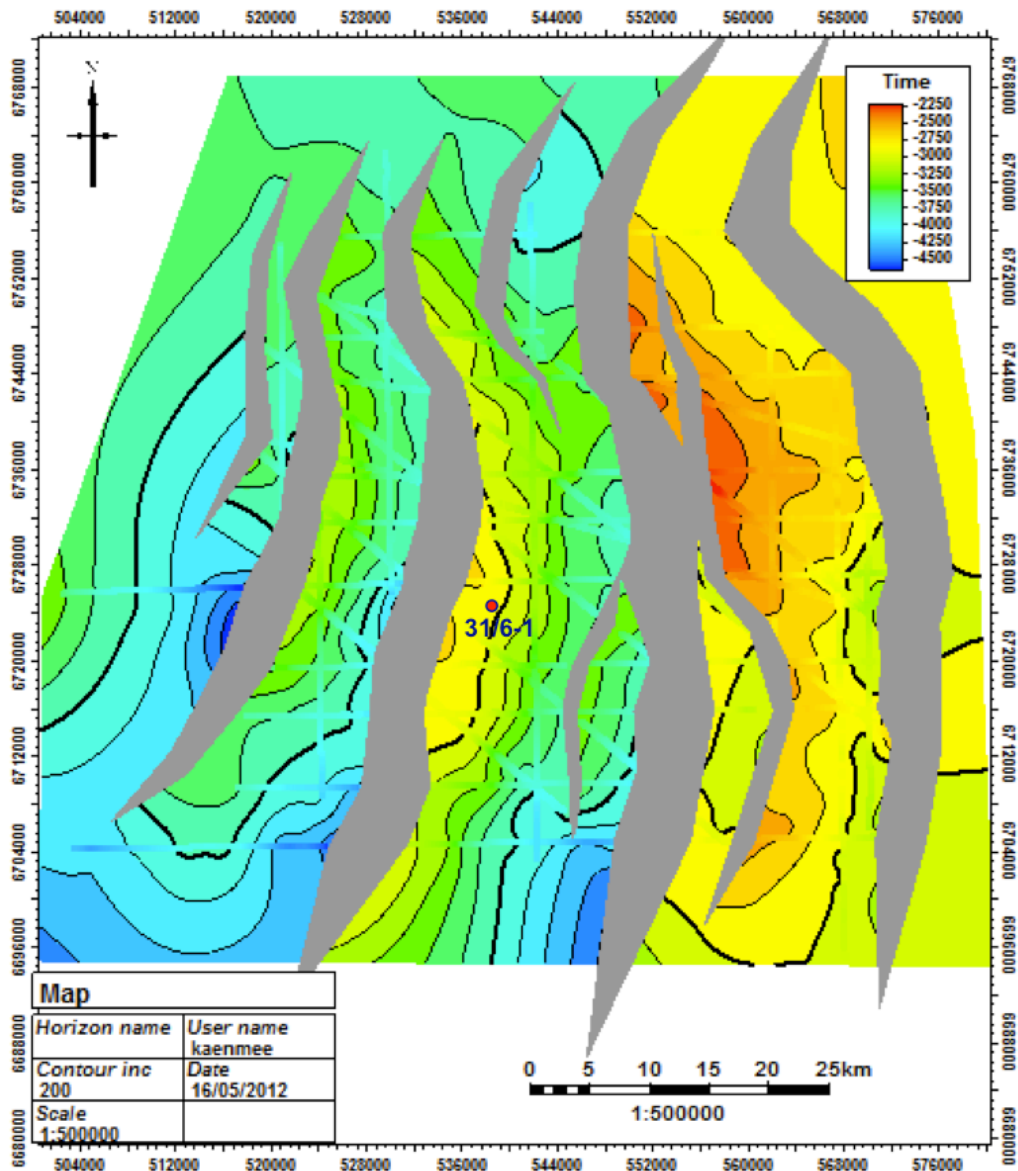


Figure 4.4 Structural time map of the Top seismic basement with well 31/6-1.

5. Discussion

5.1 Normal faulting and basin evolution

Along an isolated normal fault, the highest footwall- and deepest hanging wall topography are ideally located in the center of the fault zone, and the magnitude of these parameters decreasing towards its end (Gawthorpe and Leeder, 2000). In this thesis, the deepest reflector that has been interpreted is the Top seismic basement. This reflector is best seen along seismic section across the Horda Platform and it is not necessary the top of the crystalline basement as mentioned before in seismic interpretation section. As the top seismic basement reflector can be regarded as the base of the northern North Sea basin (within uncertainties) and existed before the rifting, it can be used to understand the evolution of normal faults in the early rift stages, and its relations to footwall uplift and hanging wall subsidence. According to the structural time map of the Top seismic basement and cross sections; a-a', b-b' and c-c' (Figure 5.1), the largest fault displacement of fault C is displayed in cross section a-a', and it decreases progressively to the north, as seen in sections b-b' and c-c'. Surface topography simultaneously shows the relatively highest and lowest elevations on the footwall and hanging wall respectively at the place where the largest fault displacement is situated. This implies that amount of the uplift and subsidence is a function of the magnitude of fault displacement. Moreover, a possible reason why the longest segment and highest displacement rate is located at the fault center on the hanging wall side is that because this central segment (e.g. segment of fault B in Figure 5.2C) is most frequently loaded by laterally adjacent segments (e.g. segments of fault A and C in Figure 5.2C). In contrast, segments located at the latest segment among many have low displacement rate and short segment (Gawthorpe and Leeder, 2000).

Furthermore, Gawthorpe and Leeder (2000) stated that basin architecture depends upon the three-dimensional evolution of basin linkage through fault propagation. The processes of fault propagation, growth, linkage between different segments and death are important tectonic factors that control basin architecture and they can be tested by using observational evidence from the earliest stages of rift development as illustrated in Figure 5.2. In the initial stage of normal fault evolution, a large number of small- and isolated-displacement normal fault segments are commonly formed and the low surface topography is influenced by fault propagation folds and surface-breaking normal fault scarps (Figure 5.2A). In the stage of fault interaction and linkage, growth and deformation in the fault array begin to become localized along major fault zones (A, B, C) caused by the stress interaction between segments (Figure 5.2B). Faults located in stress shadows begin to become inactive (X, Y, Z) (Gawthorpe and Leeder, 2000). In the last stage, the deformation is localized along major border fault zones simultaneously with formation of large half graben (Figure 5.2C). It is clearly seen that the fault displacement is become larger and larger from the initiation stage to the through-going fault zone stage. This can be used to differentiate the stages of fault presented today. For instance, the maps of the Pre-Jurassic 1 (Figure 4.2) and the Top seismic basement (Figure 4.4) show the smallest and largest width of fault polygons respectively. Therefore, the faults from the first map

can be fundamentally identified to develop in the stage of fault interaction and linkage and the latter map in the last stage of normal fault evolution.

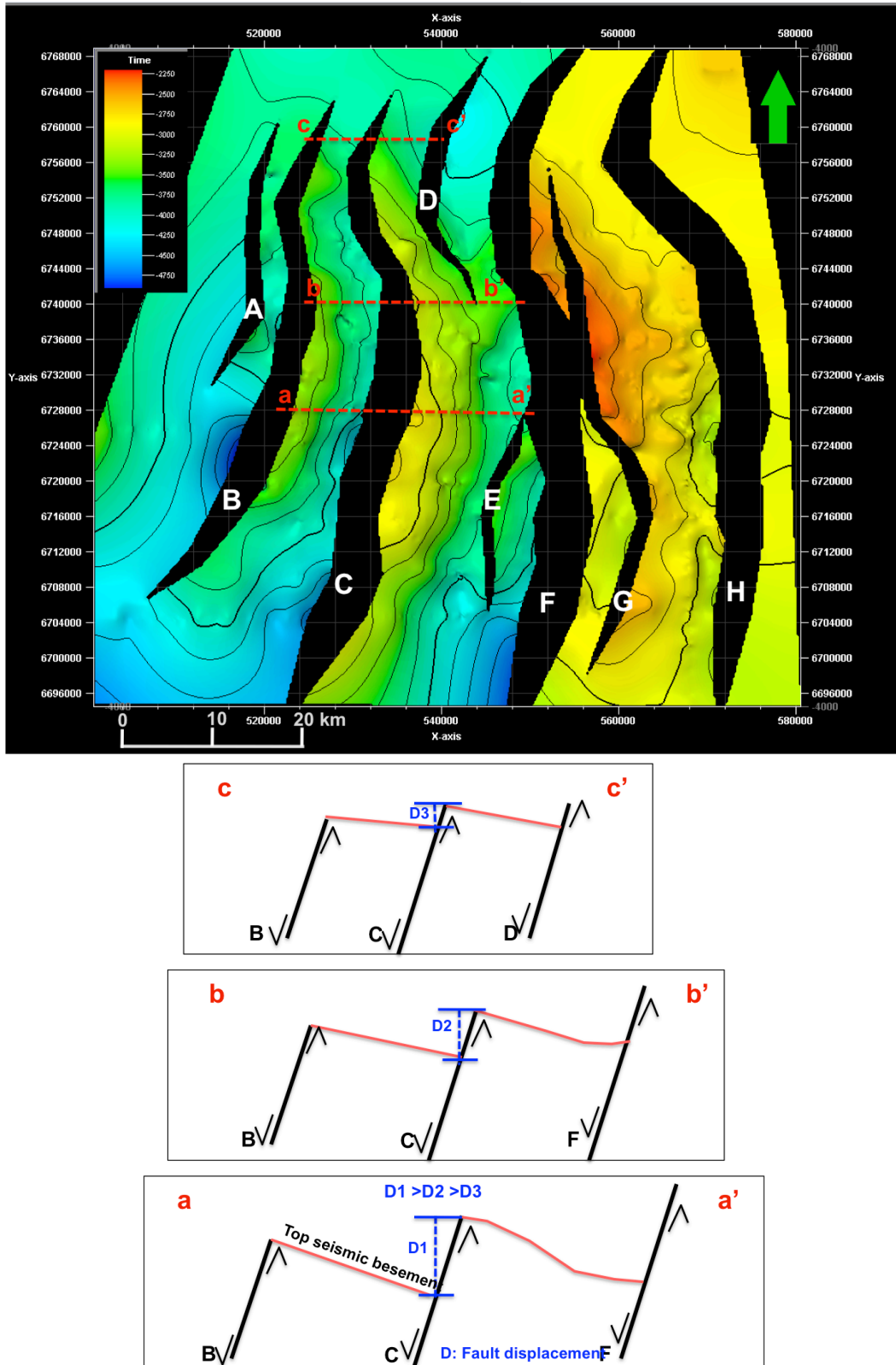


Figure 5.1 Structural time map of Top seismic basement and schematic cross-sections perpendicular to fault C, D and F, showing the largest fault displacement in a location of cross-section a-a' and decreases gradually in a location of cross-section b-b' and almost die out in a location of cross-section c-c'. Note. Features in cross-sections are not to scale.

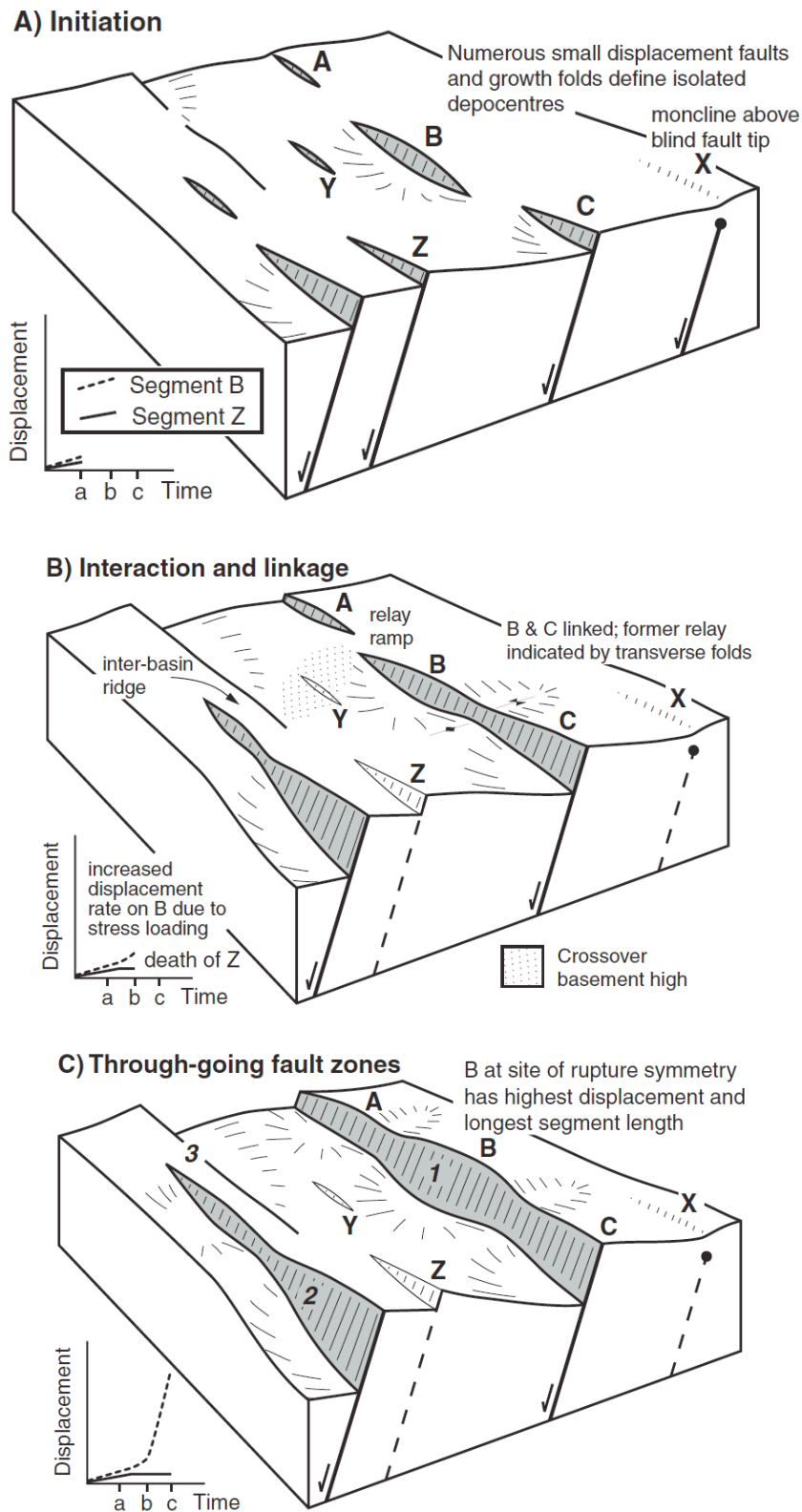


Figure 5.2 Schematic 3D evolution of a normal fault array, with graphs illustrating displacement history of fault segments B and Z. (A) Fault initiation stage, (B) Fault interaction and linkage stage, (C) Through-going fault zone stage, major half graben and graben depocentres are clearly formed. (From Gawthorpe and Leder, 2000)

In this thesis work, the structural time map of the Top seismic basement is not only used to demonstrate how a single normal fault develops through time, but also used to elaborate the

next step of fault development, which is the stage of fault interaction and linkage. This stage is associated with the relationship between the faults and the topography of the faulted surface. In Figure 5.3, on the footwall side of fault C, for example, each depressed areas, marked by syncline symbol by the red arrows, is clearly located in between the two higher elevated crests. These areas indicate the joined locations of three formerly isolated faults. In addition, slightly elevated areas, marked by the anticline symbol by blue arrows, can be also seen on the hanging wall side to support the linked location of two faults. This small degree syncline topography on footwall side and the anticline topography on hanging wall side together are introduced as a term “transverse folds” (Figure 5.2) by Gawthorpe and Leeder (2000). In addition, these transverse folds also can be observed from other faults, such as, fault B and G (Figure 5.3).

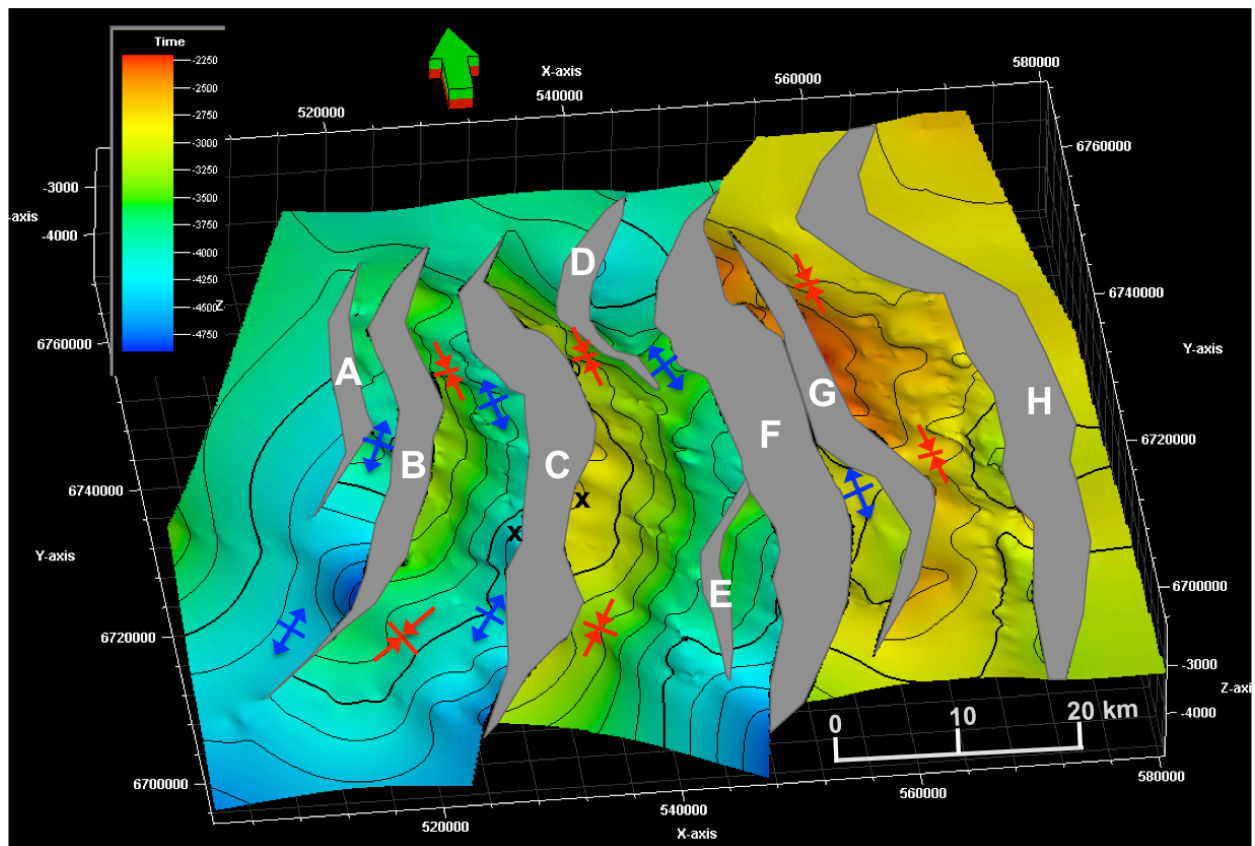


Figure 5.3 Illustration of fault linkages, for example, two synclines (red arrows) on footwalls of fault B and C indicating that at least three isolated fault segments may have merged into to each fault.

Furthermore, the activity of growing normal fault is considered to be the main factor to control the pattern of uplift and subsidence on each fault (Gawthorpe and Leeder, 2000). The growth fault is the result from fault interaction and linkage; namely, faults grow from isolated and small displacement faults to one major fault zone (Figure 5.2). These processes result in larger fault displacement and accommodation space for sediment to deposit. Moreover, the fault reactivation might have caused the larger segment, by increasing the fault heave, and led to the larger sediment load. According to the map in Figure 5.3, the highest footwall topography and deepest hanging wall topography, for example, of fault C are located in the center of fault zone, marked by “x” in Figure 5.3, indicating the center of the uplift and subsidence respectively. The longest height counts from the deepest part to the highest part across the fault plane of fault C is approximately 1000-1500 ms TWT and it is much more larger than the longest height from the

Pre-Jurassic 1 map (Figure 4.2). This implies that growing fault activity, and uplift and subsidence at the Top seismic basement is affected by the larger magnitude of extensional normal fault systems in Upper Paleozoic – Early Mesozoic period than in Late Triassic time.

Eventually, a large number of normal faults are linked and some faults may become inactive because they are located in the stress shadow zones (Gawthorpe and Leeder, 2000) such as fault D and E (Figure 5.1 and 5.3). They may be reactivated again during the later rift episode if they are in the active zones. Even though the major rift axes in the northern North Sea have been transferred from the Horda Platform to the present North Viking Graben, many workers stated that most of the faults from the Permo-Triassic rift were reactivated and rotated during the Late-Jurassic rifting as well as during the subsequent cooling. In Figure 5.4, two main trends of fault alignments in the northern North Sea are, firstly, north-south direction on the Horda Platform, central and southern part of the Øygarden Fault Zone and southern part of the North Viking Graben, and, secondly, northeast-southwest direction in the rest of the North Viking Graben, in the northern part of the Øygarden Fault Zone, the Tampen Spur and Snorre Fault Block, and the Sogn Graben. This implies that at least two major extension phases with slightly different direction occurred in the area.

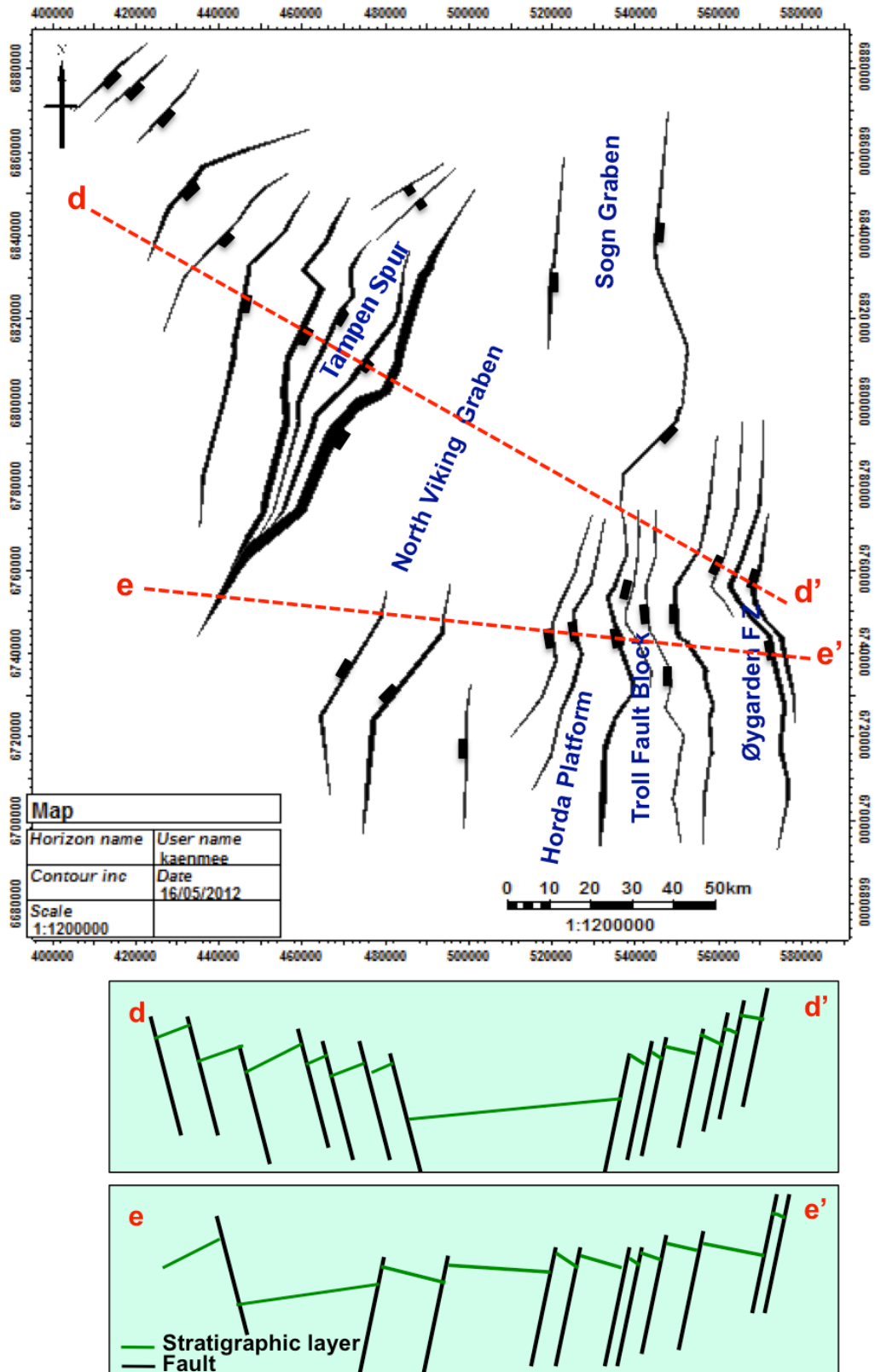


Figure 5.4 Structural framework in the northern North Sea. Two main trends of fault alignment: north-south and northeast-southwest, is shown, and cross-sections d-d' in the north and cross-section e-e' in the south are to represent the overall structures along the North Viking Graben. Note. Features in cross-sections are not to scale.

5.2 Stratigraphy and sedimentary architectures related to basin development

In the rift basin, the stratigraphy and sedimentary architectures fundamentally consisted of prerift, synrift and postrift sequences (Figure 5.5), where the latter two are the outcomes of tectonic activity such as extensional normal faulting and post-rift thermal subsidence. The prerift sequence refers to the relatively subparallel strata with comparatively constant thickness located beneath the synrift succession. The synrift succession refers to the wedge-shaped successions of strata thickening towards half-graben bounding faults on the hanging wall side. The postrift sediment is represented by a set of unrotated and unfaulted subparallel strata that sit discordantly on top of the rotated and faulted successions of synrift and prerift rocks (Figure 5.5). They are mostly bounded by an unconformity at the transition from prerift to synrift and synrift to postrift sediments. The stratigraphic importance of the basal unconformity depends on how much time the hiatus represents from one previous sequence to a new one, between, for instance, the uppermost synrift strata and the lowermost postrift strata, and how much tectonic uplift, rotation and erosion occurred in the area.

In the North Viking Graben, where the effects of the Late Jurassic rift are particularly well preserved, the unconformity located at the boundary of synrift and postrift successions is more pronounced than the unconformity situated at the boundary of prerift and synrift rocks (Figure 5.5). The potential reason why unconformity at the Early Cretaceous is stronger is that time gap from top of synrift sequence to BCU is larger, heavier weathering and erosional processes took place and results in the strongest acoustic impedance due to the large difference in rock properties above and below the unconformity (Figure 5.5).

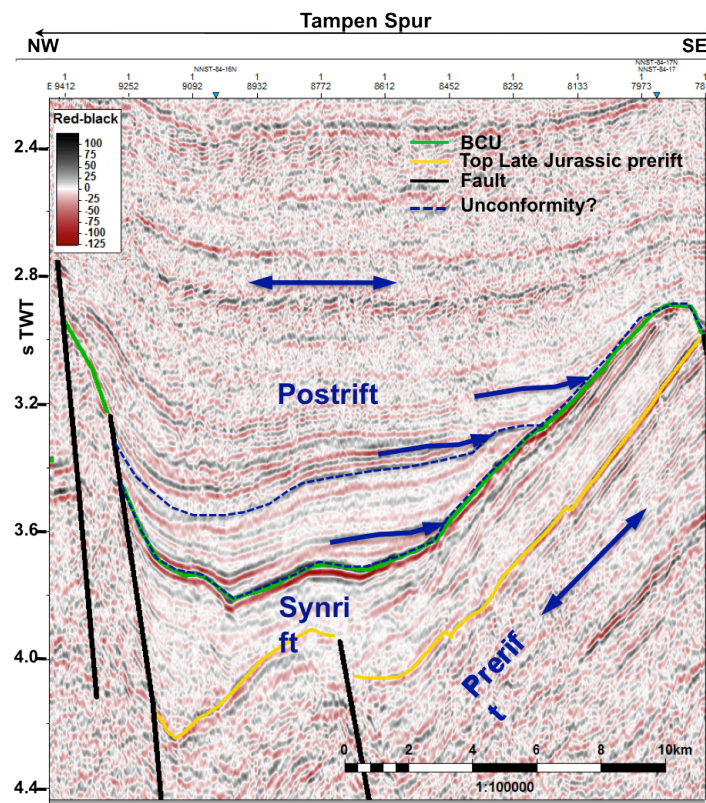


Figure 5.5 Simple illustration of sedimentary architectures in a rift basin, showing subparallel and wedge geometry in the northern part from the 2D seismic line NVGT88-08.

Furthermore, the thickness of the triangular wedge-shaped geometry of synrift sequences can be used to estimate the magnitude of the extension and basin subsidence of each rift. In comparison between the Permo-Triassic synrift and the Late Jurassic synrift successions, it is clearly seen that extension that caused the Permo-Triassic synrift is much larger than the Late Jurassic one, with the largest thickness being 1.1 sTWT (Figure 5.6) versus 0.6 sTWT (Figure 5.5), respectively. Moreover, the heaves on the half-graben bounding faults of both rifts show the concordant observations, that is, heave being 5 km (Figure 5.6) versus 1 km (Figure 5.5) on the Permo-Triassic and the Late Jurassic half grabens respectively. Therefore, the major part of extension and the greatest stretching and initial subsidence occurred during the Permo-Triassic episode and that the basin thermal subsidence of the Late Jurassic phase is for a large part due to the thermal subsidence resulting from the earlier event (Ter Voorde et al., 2000). Besides, well 31/6-1 has confirmed the age of the Permo-Triassic synrift sediments is poorly constrained by varying from Devonian to Triassic in this wedge-shaped geometry on the Horda Platform (Christiansson et al., 2000). Hence, this early rifting episode possibly has taken longer time than the Late Jurassic rift.

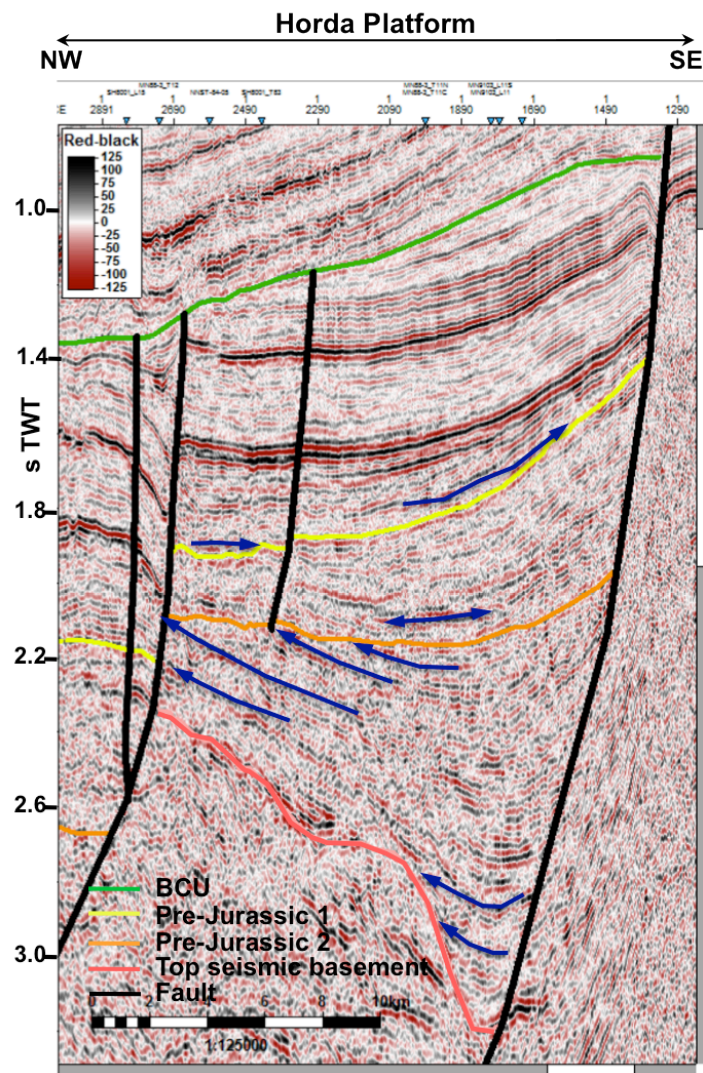


Figure 5.6 Triangular wedge geometry of synrift succession of the Permo-Triassic rift from the 2D seismic line NVGT88-05.

An Isochore map of the Permo-Triassic's synrift succession, from Top seismic basement reflector to Pre-Jurassic 2 reflector, has been generated as shown in Figure 5.7a along with cross section in northwest-southeast direction from point X to point X' in Figure 5.7b. Each wedge clearly displays the typical synrift geometry, thickening toward the bounding normal faults to the east within the block, and thickness variation across the fault blocks. This implies that the faults acted as a growth fault while rifting, resulted in larger accommodation space for sediments at the hanging wall and more initial subsidence due to a sediment load inside the segment and the activity of growing normal faults in the rift basin.

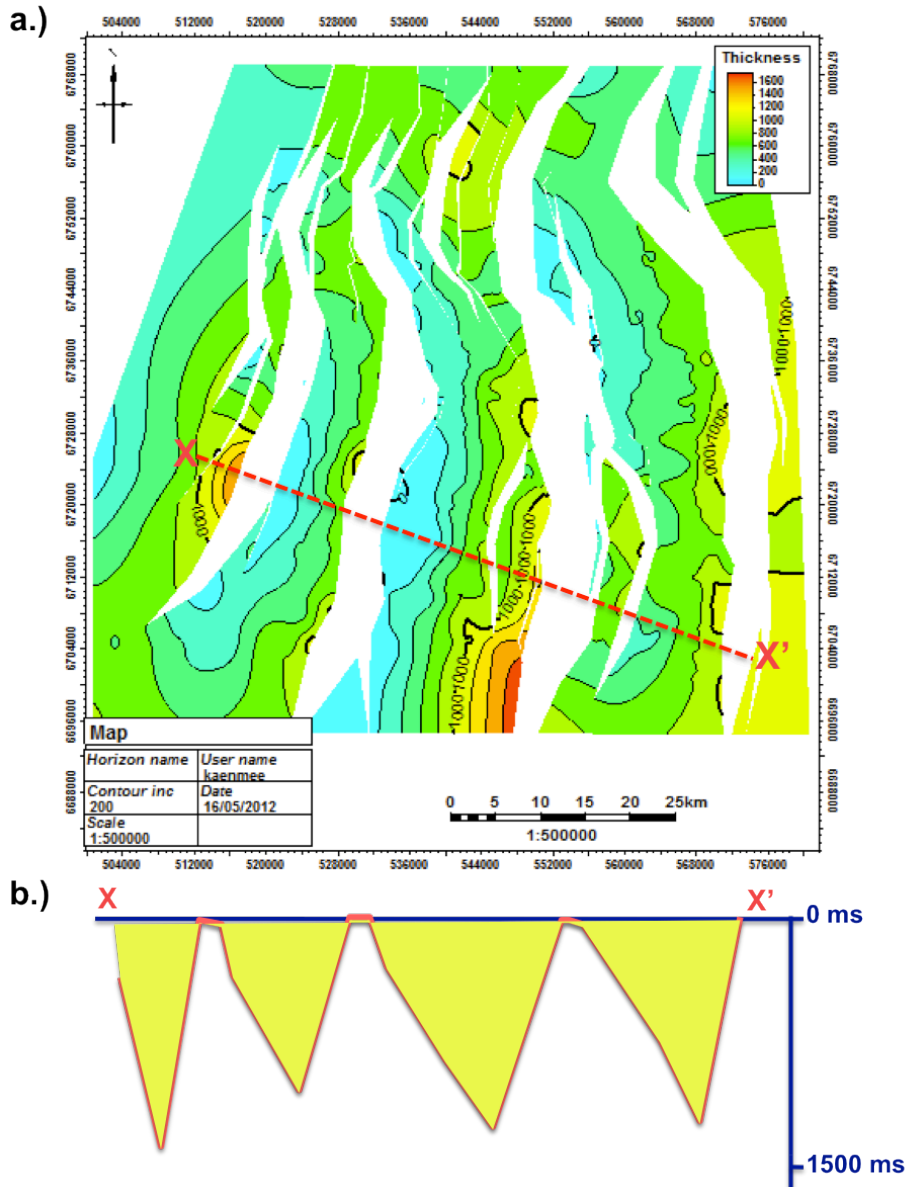


Figure 5.7 An isochore map of succession from Top seismic basement to Pre-Jurassic 2. a.) Map, b.) Cross section X-X'.

Last but not least, Ravnås et al. (2000) suggested that in the middle of the major Permo-Triassic and Late Jurassic rift episodes, the North Viking Graben has experienced several small subsidence stages and fault block rotations caused by minor extensional stages. The term “inter-rift” is used for these stages and their associated sedimentary successions. These inter-rift periods separated the major rift episodes and displayed the characteristics of short-lived rift

stages; less subsidence, less fault block rotation and less tilting are expected. A gently wedge-shaped geometry of the interval from the Pre-Jurassic 2 to the Pre-Jurassic 1 reflectors can possibly represent the inter-rift phase (Figure 5.6). Its shape is relatively less inclined and obviously smaller than the enormous wedge geometry beneath it. However, Ter Voorde et al. (2000) suggested another possible explanation for this gently inclined reflector, namely that it is a result of an interference between post-rift subsidence related to the Permo-Triassic rifting and protorift subsidence, characterized by the thermal induced domal uplift, related to the Late Jurassic rift phase. This combination might cause an extra subsidence as observed on the Horda Platform.

An isochore map of the interval from Pre-Jurassic 2 to Pre-Jurassic 1 has been constructed (Figure 5.8) across the platform area. Its cross section in west-east direction shows the gradual change in thickness within the block and also across the faults blocks and it supports the characteristics of the minor extension and/or minor subsidence. In addition, one unconformity above the BCU surface in Figure 5.5 is identified, and it might have been caused by the inter-rift stage during the stage of relative tectonic quiescence Ravnås et al. (2000).

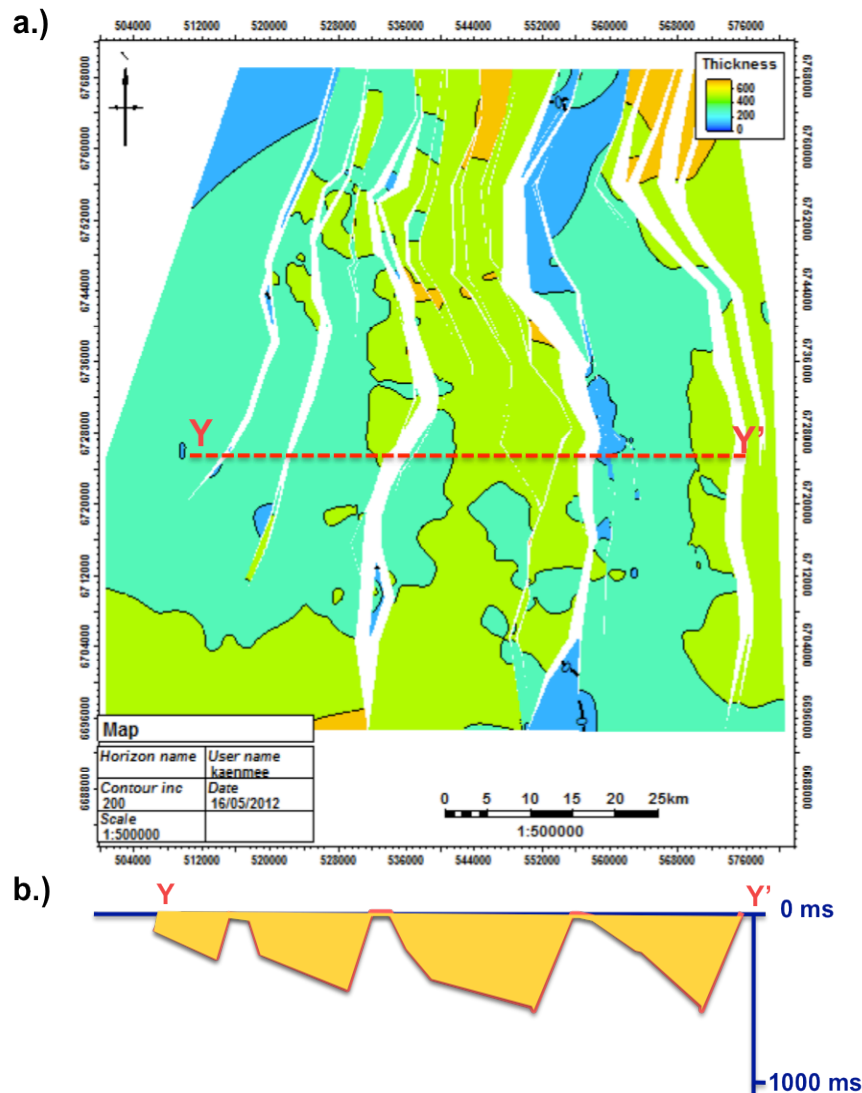


Figure 5.8 An isochore map of succession from Pre-Jurassic 2 to Pre-Jurassic 1. a.) Map, b.) Cross section Y-Y'.

5.3 Deep structure

As the North Sea basin is a failed rift basin, the last structures to form during continental extension are mostly asymmetric on a wide range of scales and detachment faulting is considered to play a principal role in the process. As a result, two stages of basin development involving detachment faults at non-tectonic margins have been described by Lister (1991), that is, (1) continental extension including the movements of steeply-dipping normal faults and shallow-dipping detachment, faults and (2) continental breakup involving the embrittlement of lithosphere resulting in seafloor spreading. Detachment faults can be seen in reflection seismic profiles, generally have listric geometries and sole out in the upper crust into shallowly to moderately dipping reflectors as an example in Figure 5.9.

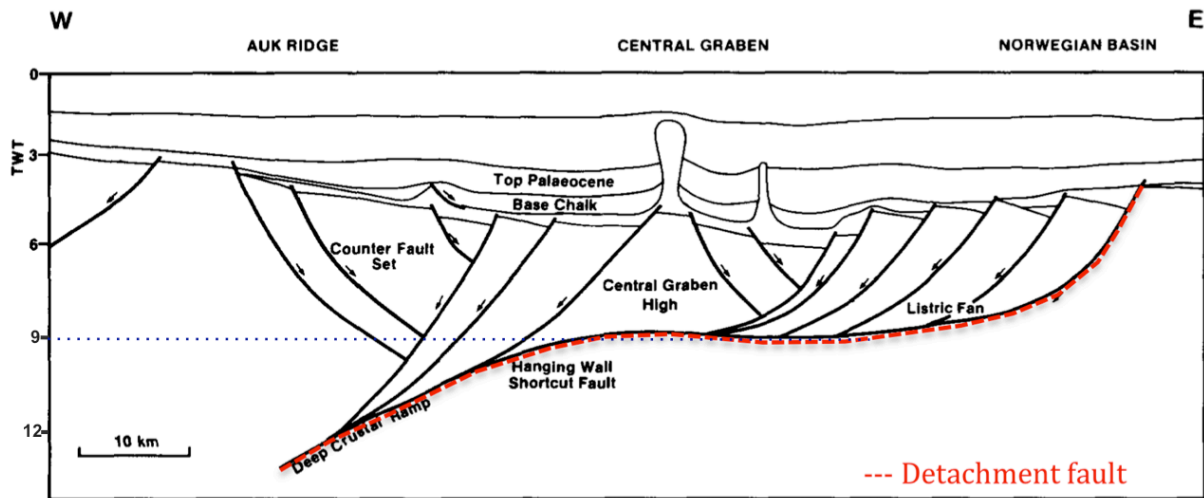


Figure 5.9 Simple illustration of detachment fault across the Central Graben, southern North Sea based on regional seismic survey (modified from Gibbs, 1984).

As seen in Figure 5.9, the detachment fault generally located approximately at 9 sTWT and moved downward to the lower crust. However, the seismic sections used in this thesis work are mostly focused on the shallow section, less than 7 sTWT (Figure 5.10). Therefore, it is very difficult to identify the detachment fault because of a lack of deep seismic profiles even on the platform area as shown in Figure 4.1 and 5.10. However, another interesting structures can be identical, for example, a possible older fault plane from the early stage of continental extension as shown as black dashed line in Figure 5.11. As it took place in the northern North Sea, a term “the first rifting normal fault” is applied to call this fault. The dipping angle of this normal fault plane is obviously gentler than the younger faults, referred to a term “the second rifting normal faults”, above it. The possible reason to explain this phenomenon is that this gentle-dipping fault plane used to be steeply dipping normal fault in the rifting stage but it was rotated and reactivated later during the younger rifting phase. The alternative likely possibility to cause the gentler dip of fault at depth is due to a velocity effect, namely, velocity commonly increases with depth, and rapid changes in velocity give rise to kinks in dipping reflectors such as fault-plane reflectors. However, no well logs have been used in this thesis to validate the interpretation. Therefore, this issue is still inconclusive.

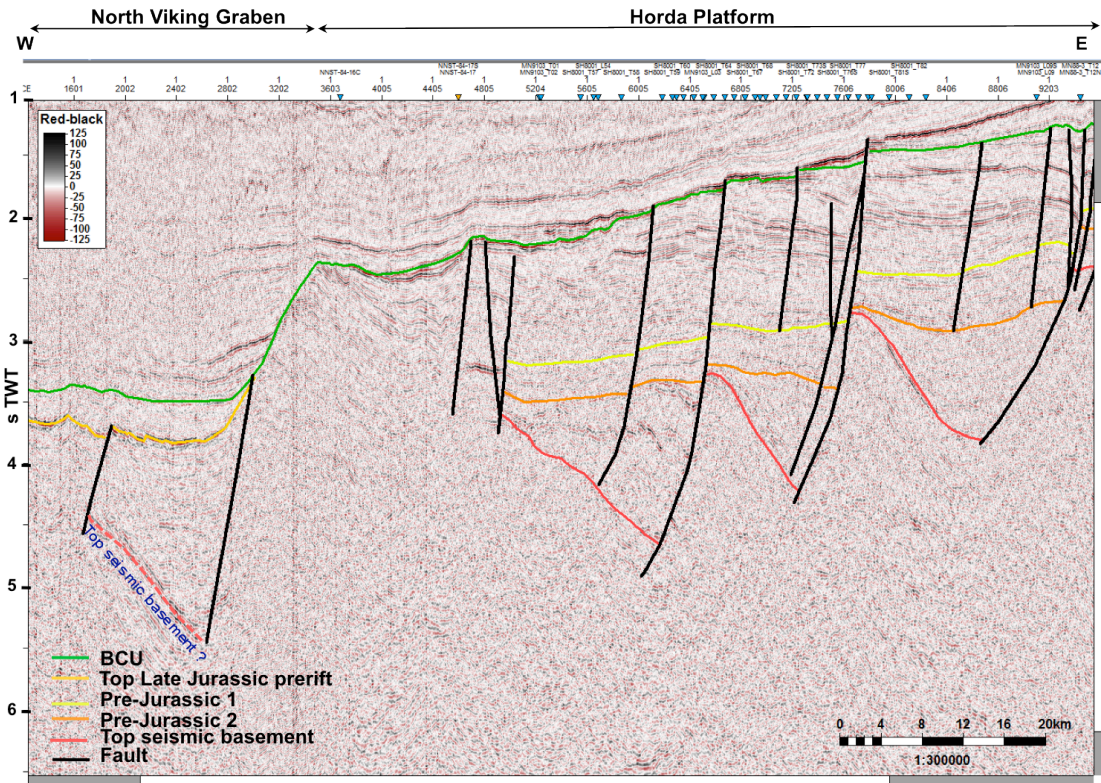


Figure 5.10 Examples of the subsurface structures under the Horda Platform in the northern North Sea from the 2D seismic line NNST84-05. Note. Deeper section, 4-6.5 sTWT, shows less seismic resolution than the shallower part, therefore, detachment faults is not able to identified on this section. Possible Top seismic basement is also displayed on the lower left of the figure.

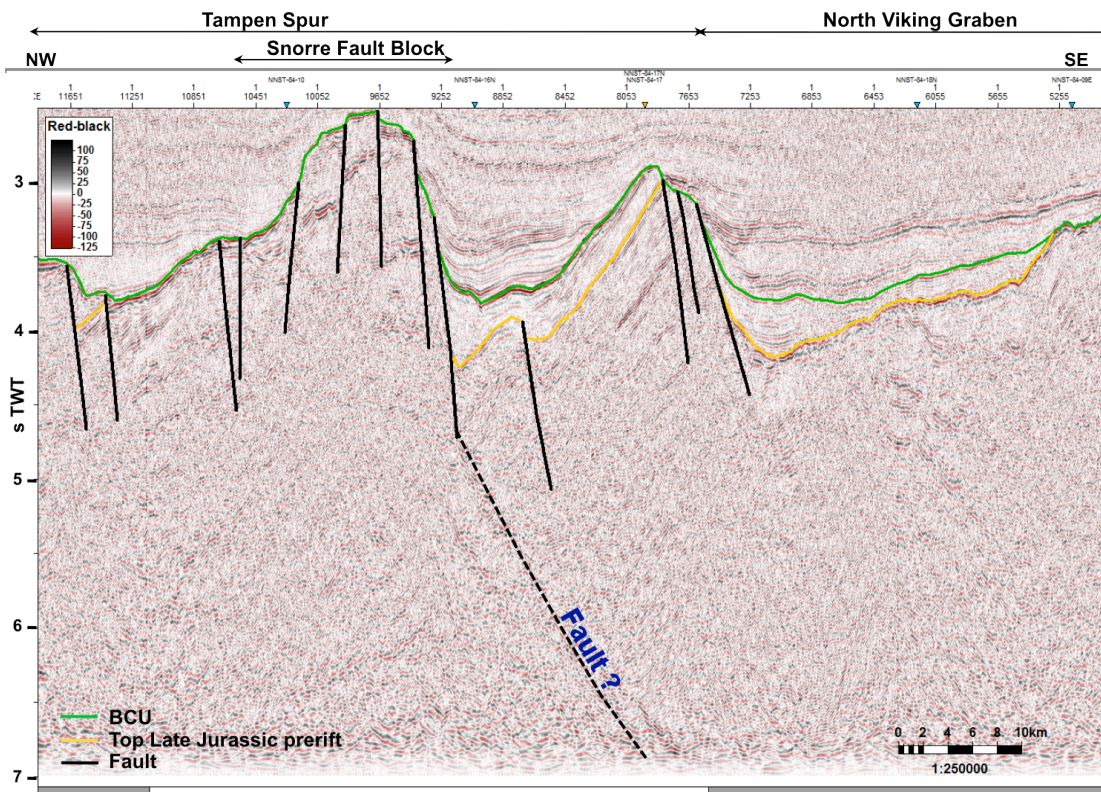


Figure 5.11 An example of the possible first rifting normal fault in the northern North Sea from the 2D seismic line NVGTI92-106.

However, these gentler- and steeper-fault plane patterns have been identified as a typical fault system of the extensional rift basin as additionally shown in Figure 4.1 and 5.10 west-dipping normal faults seem to have large fault displacement and penetrate continuously from base of the BCU through the Top seismic basement reflectors. However, they truly can be divided into two groups: first, a younger fault which is the group that has steeper fault plane located in the upper part of the section from the BCU to the Pre-Jurassic 1 reflectors, secondly, an older fault group with listric shape and gentler dip located at the lower part of the section from the Pre-Jurassic 1 to the Top seismic basement reflector. All things considered, the fault development in the rift basin can be concluded as repeated series of fault reactivation (Figure 5.12).

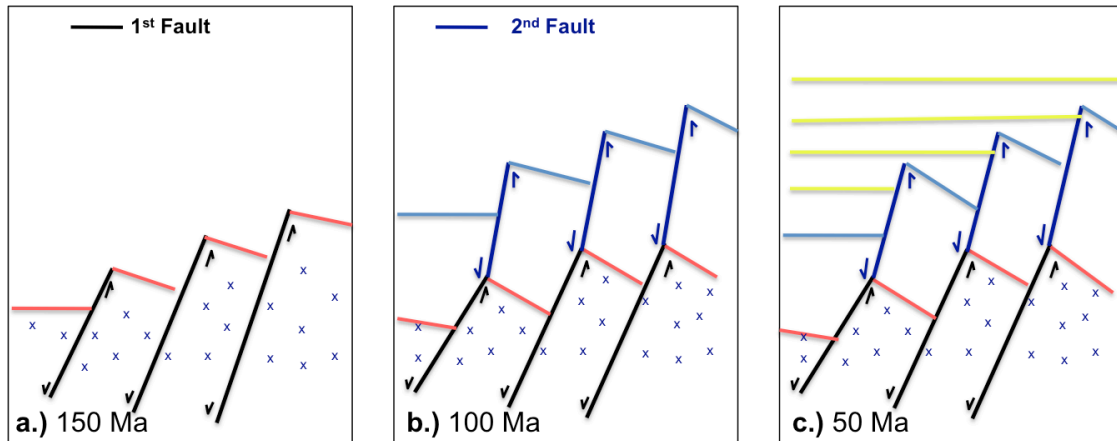


Figure 5.12 Simple illustration of fault development in rift basin. a.) Early stage of extensional normal fault system, b.) After the first fault reactivation, c.) Faults after postrift stage as displayed in present.

In addition to the wedge-shaped geometry in the graben area, another synrift geometry is identified in the interior graben area on two seismic sections of line NNST84-05 and NNST84-04 in the southern part of the North Viking Graben (Figure 5.10). They simply show the typical synrift geometry but possibly have formed in the different tectonic events. Furthermore, this configuration is located at the triple junction of changing in fault trend directions from north-south trend to northeast-southwest trend. According to its depth and geometry, Ter Voorde et al. (2000) stated that it perhaps was formed by a thermal subsidence of the Permo-Triassic rift, the onset of Jurassic succession. One possible way to solve this unclear event is to drill the wells on both locations and/or conduct the conventional coring and compare the age of sediments by performing special core sample analysis.

6. Conclusions

As the Base Cretaceous Unconformity covers most of the northern North Sea: the Øygarden Fault Zone, the Troll Fault Block, the North Viking Graben, the Tampen Spur, the Snorre Fault Block, the Sogn Graben and the Horda Platform, its structural time map, is used to derive the picture of post-structural framework (i.e. the large-scale basin architecture) of a rift basin and to locate essential structures in the deeper sections.

Three main reflectors (Pre-Jurassic 1, Pre-Jurassic 2 and Top seismic basement) located beneath the Base Cretaceous Unconformity on the Horda Platform, and have been interpreted using 2D seismic reflection data. These three reflectors have been studied in order to investigate in detail the displacement gradients and possible linkage of the early fault system under the Horda Platform, and to evaluate their effect on the large-scale sediment architecture. A main reason to work on the structures under the Horda Platform is due to the fact that these structures are believed to have existed already in the early stages of the northern North Sea basin development.

The extensional normal fault systems of both the Permo-Triassic and the Late Jurassic rifts are considered a key control on the geological structures and sedimentary architecture of the region as presently seen. The basin evolution related the Permo-Triassic rifting is most pronounced on the eastern part of the Horda platform where its synrift geometry is obviously seen with the huge segment length and largest uplift explainable by a flexural stretching model. The rift axis is transferred to position at base of the Viking graben during the Late-Jurassic rifting with the smaller magnitude of extension than the Permo-Triassic as clearly seen by the less thickness of the synrift geometry. However, the structural evolution of normal faults and the basin architecture under the Horda Platform is particularly affected by the complex interaction of fault linkage, fault propagation, fault growth, and death of fault through times from the early stage to the final stage of the basin development. Apart from the effects of major tectonic controls, additionally, non-tectonic parameters, such as climate, sea or lake level changes, and differences in amount and type of sediment supply, should be taken into account to influence the stratigraphic and sedimentation patterns in the basin.

7. References

- Christiansson, P., Faleide, I. J. & Berge, A. M. (2000), *Crustal structure in the northern North Sea: an integrated geophysical study*. Geological Society, London, Special Publications, January 1, 2000. v.167, **p.15-40**, doi 10.1144/ GSL.SP.2000.167.01.07
- Coward, M. P., Dewey, J. F., Hemton, M. & Holroyd, J. (2003), Tectonic evolution. **p. 17-33** in *The Millennium Atlas: petroleum geology of the central and northern North Sea*. Evan, D., Graham, C., Armour, A., & Bathurst, P. (editors and coordinators). (London: The Geological Society of London.)
- Cowie, P. A. (1998), *Normal fault growth in three-dimensions in continental and oceanic crust, in Faulting and Magmatism at Mid-Ocean Ridges*: Geophysical Monograph 106, American Geophysical Union, **p. 325-348**.
- Gawthorpe, R. L., Fraser A. J., Collier, R. E. Ll. (1994), *Sequence stratigraphy in active extensional basins: implications for the interpretation of ancient basin-fills*. Marine and Petroleum Geology (1994) 11, **p. 642-658**.
- Gawthorpe, R. L., Sharp, I., Underhill, J. R., and Gupta, S. (1997), *Linked sequence stratigraphic and structural evolution of propagating normal faults*: Geology, v. 25, **p. 795-798**.
- Gawthorpe, R. L. & Leeder M. R. (2000), *Tectono-sedimentary evolution of active extensional basins*. Basin Research (2000) 12, **p.195-218**.
- Gibbs, A. D. (1984), *Structural evolution of extensional basin margins*. Journal of the Geological Society 1984; v. 141; **p. 609-620** doi: 10.1144/gsjgs.141.4.0609.
- Hallam, A. (1971), Extensional tectonics in the northernmost North Sea: rifting, uplift erosion, and footwall collapse in Late Provinciality in Jurassic faunas in relation to facies and paleogeography. In: Middlemiss, F.A. & Rawson, P.F. (eds) Faunal Provinces in Space and Time. Geological Journal Special Issue, 4, **p. 129-152**.
- Heybroek, P., Haanstra, U. & Erdman, D.A. (1967), Observations on the geology of the North Sea area. In: Proceedings, 7th World Petroleum Congress (Mexico). John Wiley & Sons, Chichester, 2, **p. 905-916**.
- Kyrkjebø, R., Gabrielsen, R. H., Faleide, J. I. (2004), *Unconformities related to the Jurassic-Cretaceous synrift-post-rift transition of the northern North Sea*. Journal of the Geological Society, London, Vol. 161, 2004, **p. 1-17**.
- Lister, G. S., M. A. Etheridge, and P. A. Symonds (1991), *Detachment models for the formation of passive continental margins*, Tectonics, 10, **p. 1038- 1064**, doi:10.1029/90TC01007.

- Mosar, J., Eide, E. A., Osmundsen, P.T., Sommaruga, A. & Torsvik, T.H. (2002), *Greenland-Norway separation: A geodynamic model for the North Atlantic*. Norwegian Journal of Geology 82, p. **282-299**. Trondheim. ISSN 029-196X.
- Park, R.G. (1997). *Foundations of Structural Geology*. London: Chapman & Hall. 202 p.
- Ravnås, R., Nøttvedt, A., Steel, R. J. & Windelstad, J. (2000), *Syn-rift sedimentary architectures in the Northern North Sea*. Geological Society, London, Special Publications, v.167, p.**133-177**, doi 10.1144/ GSL.SP.2000.167.01.07.
- Rawson, P.F. & Riley, L.A. (1982), Latest Jurassic–early Cretaceous events and the ‘Late Cimmerian Unconformity’ in North Sea Area. AAPG Bulletin, 66, p. **2628–2648**.
- Ter Voorde, M., Færseth, R. B., Gabrielsen, R. H. & Cloetingh, A. A. P. L. (2000), *Repeated lithosphere extension in the northern Viking Graben: a coupled or a decoupled rheology?*. Geological Society, London, Special Publications, v.167, p.**59-81**, doi 10.1144/ GSL.SP.2000.167.01.07
- Zanella, E., & Coward, M. P. (2003). Structural framework. p. **45-59** in *The Millennium Atlas: petroleum geology of the central and northern North Sea*. Evan, D., Graham, C., Armour, A., & Bathurst, P. (editors and coordinators). (London: The Geological Society of London.)
- Ziegler, P.A. (1990), Geological Atlas of Western and Central Europe. Shell International, The Hague.

¹<http://en.wikipedia.org/wiki/Unconformity>

²Lamont -Doherty Earth Observatory, Columbia University webpage: <http://www.ldeo.columbia.edu/~polsen/nbcp/breakupintro.html>